Comparative Assessment of HIPPI Normal Conducting Structures

C. Plostinar (Editor)

Rutherford Appleton Laboratory, UK

Abstract

Over the last five years important developments needed for high intensity proton linacs have been made possible through the HIPPI collaboration. In this report we present a comprehensive comparative assessment of five normal conducting accelerating structures considered by the HIPPI Work Package 2 collaborators: the DTL (Drift Tube Linac), the CH-DTL (Crossbar H-mode DTL), the CCDTL (Cell Coupled DTL), the PIMS (π-mode Structure) and the SCL (Side Coupled Linac).

Table of Contents

1. Introduction

With increasing demand from the physics community for secondary particle beams, a number of European laboratories have followed separate development programmes for high intensity proton linacs. The linacs are designed to deliver primary beam onto a target, and topics under study include normal conducting and superconducting accelerating structures, beam dynamics and code development, chopping methods, ion sources and radio frequency quadrupole (RFQ) development.

The HIPPI Joint Research Activity [1] was aimed at developing a common European technology base for the construction of high intensity pulsed linear accelerators. It coordinated the work on the above topics into a systematic study of technological alternatives up to an energy of 200 MeV. The proposed R&D activities achieved an excellent level of competence and facilitated substantial improvement of accelerator complexes at European Laboratories.

1.1. HIPPI Work Package 2 (WP2)– Normal Conducting Accelerating Structures

HIPPI Work Package 2 coordinated the development of normal conducting accelerating cavities for the above mentioned energy range. Three main European projects have benefited most from the WP2 collaboration:

- The Linac4 accelerator at CERN is a 160 MeV H^- linac presently under construction. It is the first phase of a proposed staged upgrade of the CERN proton injector complex.
- The 70 MeV proton injector for the FAIR project at GSI.
- The ~200 MeV H^- Linac at Rutherford Appleton Laboratory (RAL) currently proposed as a possible replacement for the ISIS proton injector.

Normal conducting RF structures are good candidates for beam acceleration in a pulsed proton linac, up to an energy exceeding 100 MeV [2]. This is especially true if this is the final linac energy, as in the case of the three projects under consideration, because investment in cryogenic infrastructure can be avoided. From a beam dynamics point of view, depending on the subsequent accelerator chain, the requirements can be quite different. In the case of CERN, Linac4 has to be able, with a high duty factor, to deliver a beam quality that is adequate both

for injection in the PS Booster and for a cascaded high energy superconducting linac (i.e. a beam without halo) [3].

Different requirements for the proposed linac projects led to different choices of RF structures and beam dynamics, which were developed in parallel and experimentally compared to help optimise the designs. In the case of CERN, a classical beam dynamics was adopted, and the types of structures considered are the Drift Tube Linac (Alvarez DTL) for the energy range from 3 to 50 MeV, Coupled Cavity Drift Tube Linac (CCDTL) for 50 to 95 MeV and the π-mode Structure (PIMS) above 95 MeV. A Side Coupled Linac (SCL) was also analysed as a possible alternative to the PIMS.

For the GSI linac with a final energy of approximately 70 MeV, the "KONUS" beam dynamics was adopted, with the use of H-mode structures over the whole length of the linac (Crossbar H-mode DTL – CH-DTL).

For the RAL linac several schemes are under study with the most advanced design consisting of a Drift Tube Linac up to ~80 MeV followed by a Side Coupled Linac up to the final energy.

In order to validate the technological choices and help select the economical optimum, prototype model cavities have been designed, built and tested for the above mentioned structures. The simultaneous development of these complementary structures in a single Joint Research Activity (JRA) has resulted in an optimum use of the existing infrastructure (high power RF test places, computer codes, etc.), a broadening of the knowledge available to every individual contributor, and finally in a more strongly justified choice of technological solutions for any future high intensity proton linac.

2. Comparison Criteria

Several general criteria can be used to describe normal conducting accelerating cavities. For the HIPPI structures the aim is not only to generate an evaluation based on their theoretical RF properties, but also to discuss the effect on the beam quality, give a general overview on the technologies and the precisions involved, the field stability to be achieved and the tuning procedure as well as the structure's sensitivity to RF errors. We believe that taking all these criteria into account represents a more accurate way of describing the RF properties of normal conducting cavities as well as the complexity and effort involved in the design and the manufacture process.

2.1. RF Properties and Power Efficiency

Several figures of merit are used to characterize accelerating cavities and are generally applied as guidelines by linac designers.

Power Efficiency. For normal conducting accelerating cavities, one of the main objectives in cavity design is to choose a geometry to maximize the power efficiency of the structure, that is why it is convenient to define the *shunt impedance* as a measure of the effectiveness of producing an axial voltage V_0 for a given power dissipated P_0 [4]. The shunt impedance is independent of the excitation level of the cavity, it is usually expressed in MΩ and is defined by:

$$r_s = \frac{V_0^2}{P_0}$$

Since we are interested in maximizing the particle energy gain per unit of power dissipation, it is useful to define an effective shunt impedance. This takes into account the fact that as the particle crosses the gap the field is also varying and as a result the cavity is less efficient and the energy gain is only a fraction of the peak voltage in the gap:

$$r = {}_s \cdot T^2$$

where T is the transit-time factor.

The figure of merit that we will be using to describe the power efficiency of the structures is the *effective shunt impedance per unit length*, ZT^2, a "real estate" shunt impedance which is independent of both the field level and cavity length:

$$ZT^2 = \frac{\text{“}}{L} = \frac{\text{‘}E_0T)^2}{P_0 / L}$$

Kilpatrick Limit. At sufficiently high field, normal conducting copper cavities will suffer electric breakdown that limits the maximum electric field achievable. The Kilpatrick limit defines empirically the conditions that would result in breakdown-free operation, relating the operating frequency with the maximum achievable electric field [5].

$$f = .64E_k^2 e^{-.5/E_k}$$

f (MHz) – frequency

E_k (MV/m) – Kilpatrick limit

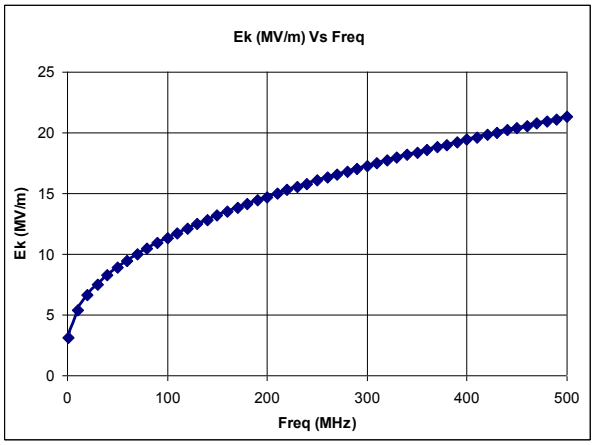

Figure 1. The Kilpatrick field variation with frequency.

Although modern RF cavities have successfully been operated at fields much higher than $1E_k$, the Kilpatrick limit remains a figure of merit in RF design (see Figure 1).

In addition to these figures of merit, the RF properties of the cavities will be characterized by several other parameters: the RF peak power, the electric field gradient as well as the "real estate" gradient and the RF power over energy gain, a parameter giving the power required (kW) for a 1 MeV increase in energy.

2.2. Beam Quality

Beam dynamics considerations have an influence on the choice of the structure parameters from the conception stage of any linac design. As a general rule, the main guidelines followed are the control of losses, the minimisation of emittance growth as well as the control of the halo development. In order to achieve these, several criteria have been taken into account by every HIPPI linac project:

- A zero-current phase advance always below 90° for stability.

- A phase advance ratio (longitudinal to transverse) between 0.5 and 0.8 in order to avoid emittance exchange between the longitudinal and transverse planes.
- A smooth variation of the transverse and longitudinal phase advance per meter.

The performance of each structure has been assessed by tracking a generated test beam distribution starting at the entrance (used to check the structure with and without space charge), as well as more realistic matched distributions. The beam loss, the input and output emittances, as well as the emittance growth have been monitored and have allowed a global optimization of the accelerating structures in the context of a complex machine.

2.3. Technologies

A third factor we have taken into account includes a list of technologies and precision requirements involved in building a proton linac suitable for high intensity operation. It is always possible to design a state of the art machine that demands very tight machining and regulation tolerances (over-design), but this approach can lead to very high costs, that is why we believe a more comprehensive assessment has comparison terms for complexity and effort. Some of the most common technologies used in manufacturing normal conducting structures include:

- Copper plating
- Welding
- Brazing
- Machining and mechanical construction, etc.

In addition to this the required mechanical accuracies will be listed as well as any operational experience in a high intensity regime. Examples where the structures have been used for high intensity applications will help make a difference between those that have been proposed for high intensity operation and those that have already demonstrated this capability.

2.4. Tuning

The tuning of accelerating NC tanks has three aspects: frequency tuning, field profile tuning and stability tuning against perturbation. For each individual structure the overall tuning procedure will be described, as well as the field and frequency stability to be achieved.

2.5. Sensitivity to RF Errors

RF errors at the klystron level translate directly into accelerating voltage errors which in turn will have an impact on the beam quality that is why in high-current proton linacs, precise tuning of RF amplitude and phase is indispensable to reduce uncontrolled beam loss and beam-quality deterioration. In general, tuning goals are set to ±1° in RF phase and ±1% in amplitude at the klystron level. However, the effects of these RF errors can be different for different structure types and will be reviewed for each accelerating cavity examined.

3. Accelerating Structures

The following five normal conducting accelerating structures are being considered as potential candidates for the three HIPPI linac projects: the DTL (Drift Tube Linac), the CCDTL (Coupled Cavity Drift Tube Linac), the SCL (Side Coupled Linac), the CH-DTL (the "Crossbar H-type" DTL) and the PIMS (PI-mode structure).

3.1. The Drift Tube Linac – DTL

The classic drift tube linac is the standard accelerating structure generally used for the lower energy part of proton linacs as its RF efficiency is drastically decreasing at energies approaching 100 MeV. Many DTLs have been in continuous operation for decades in machines around the world, like the Linac2 injector at CERN or the ISIS linac at RAL, while new high intensity linacs recently commissioned include modern DTL designs like the J-PARC project in Japan (3 – 50 MeV) or the SNS at Oakridge in the US (2.5 – 87 MeV).

RF Properties and Power Efficiency

The DTL for the new linear accelerator Linac4 at CERN will accelerate H^- ion beams of up to 40 mA average pulse current from 3 to 50 MeV using three accelerating tanks [6]. It is designed to operate at 352.2 MHz and at duty cycles of up to 10 %, if required by future physics programmes. The accelerating field is 3.2 MV/m over the entire length of the DTL section. Permanent magnet quadrupoles (PMQs) are used as focusing elements, having the advantage of small size at medium magnetic gradients without the need for current supply wires or power converters [7], [8].

On the other hand, the DTL for the proposed ~200 MeV RAL linac will operate at 324 MHz and will accelerate a 30 mA (after chopping) H^- ion beam up to ~75 MeV using four accelerating tanks. It utilises compact PMQs, the repetition rate is 30 Hz and the duty cycle for the extent of the beam pulse is ~2.1%. The RAL linac however, is in a very early design stage and many of these parameters are not yet fixed and are likely to change [9], [10]. A summary of the RF properties for the Linac4 and RAL DTLs is presented in Table 1.

Table 1. DTL RF Properties

		LINAC4 DTL		RAL DTL
	Tank 1	Tank 2	Tank 3	
Energy Gain (MeV)	9.19	19.64	18.43	71.8
Total RF Peak Power / Copper Power (MW)*	0.95 / 0.58	1.92 / 1.13	1.85 / 1.11	7.67 / 5.52
E_0 (MV/m)	3.2	3.2	3.2	2.71 to 2.9
ϕ_s (deg)	-30 to -20	-20	-20	-42 to -21
Maximum surface electric field (Kilp)	1.6	1.4	1.3	1.44
Frequency (MHz)		352.2		324
"Real estate" gradient (MV/m)		2.5		1.96
RF Power*/Energy Gain (kW/MeV) – without beam loading		60		76.8
ZTT (MOhm/m)* – Min/Max		30 - 56		25 - 45
Total length (m)		18.7		36.6

* Calculated ZTT values scaled down to 80% to take into account additional losses. Consistently, the power dissipation values have been scaled up by a factor of 1.25.

Assuming the electro-magnetic design aims at optimizing the shunt impedance for a single DTL cell, increasing the drift tube face angle will help concentrate the axial electric field and increase the structure's efficiency. Reducing the gap will increase the transit time factor, thus the effective shunt impedance. However, the face angle defines the geometry of the drift tube, whose shape is not a free parameter, as it has to hold a quadrupole magnet inside. At the same time, the gap length cannot be made too small as it will limit the voltage gain for a given peak surface electric field, increasing the Kilpatrick factor.

As it can be seen, the optimisation process has to take many factors into consideration, and for a single DTL cavity this can be done in several steps. First the drift tube geometry is chosen so that it can accommodate quadrupole magnets; then the gap length and the drift tube shape are optimized in order to maximise the r/Q and keep the Kilpatrick factor within reasonable limits; and finally the overall geometry is adjusted in order to maximise the quality factor Q, while retuning the cavity to the nominal resonant frequency. Although the aperture radius has a strong influence on the shunt impedance, its choice is usually dictated by beam dynamics considerations and in Linac4 a constant ratio between the beam pipe and the RMS beam size of

~7 was kept throughout the whole linac. After the initial single cell has been calculated, the process can go one step further and an entire succession of cells forming a tank will be optimised, thus creating an even more complex multi-dimensional design space.

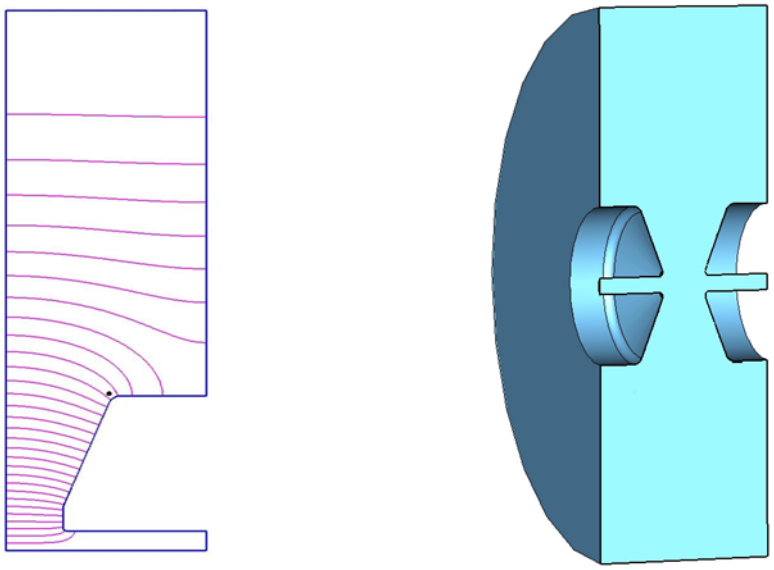

Figure 2. Basic half cell DTL 2D geometry (from Superfish) [11] and 3D geometry (from CST Microwave Studio [12]).

The results of shunt impedance calculations performed with Superfish are presented in Figure 3. To take into account additional losses coming from surface roughness, imperfections, tuners, coupling slots, etc. linac designers scale the predicted theoretical results by different values. For the DTL case, a 20% reduction in Shunt Impedance was considered appropriate. This scaling doesn't include the contribution of the post-couplers.

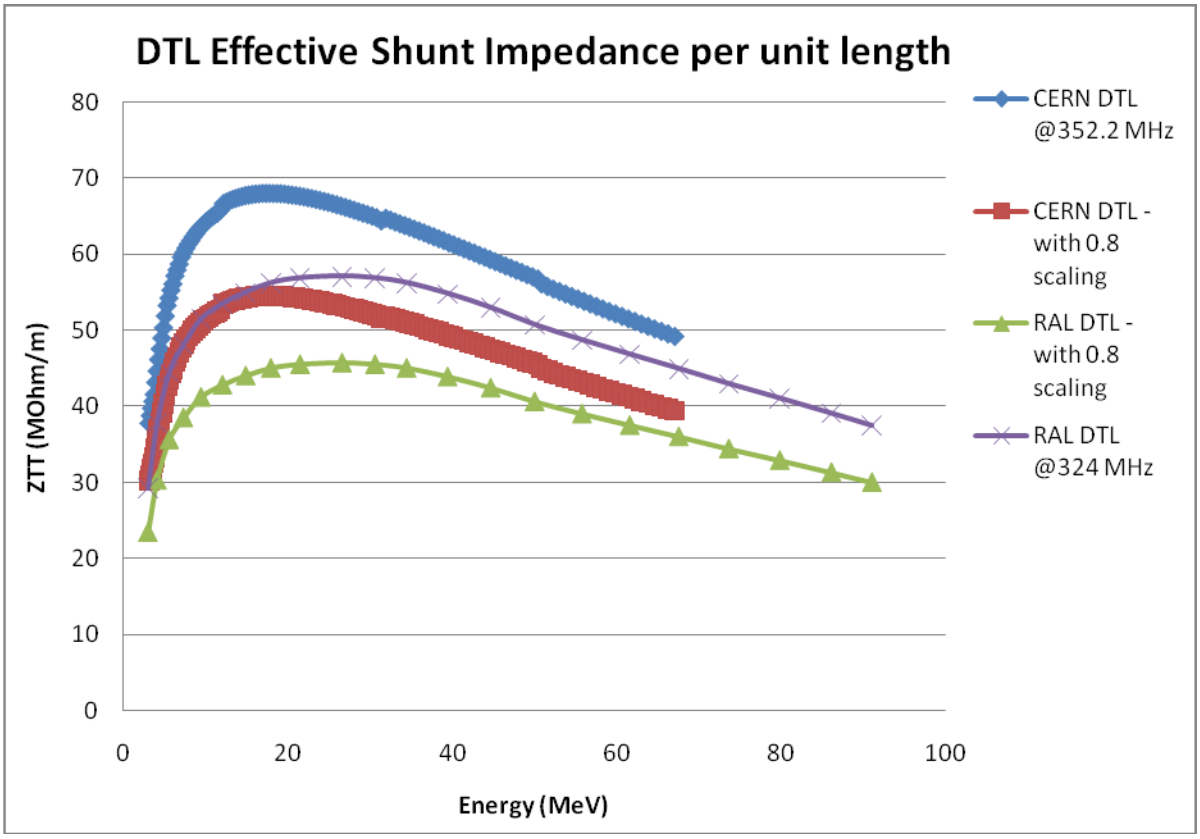

Figure 3. Effective Shunt Impedance per unit length for the DTL structure

Beam Dynamics

The overall design philosophy of Linac4 aimed for a good transmission (<1W/m losses) and minimum emittance growth. Four different DTL designs have been proposed [13]. The baseline design has a constant electric field and synchronous phase profile, a FFDD reference focusing scheme in the first tank followed by a FODO lattice in tanks 2 and 3. The reason for this choice is purely technical as it was not sure whether the higher integrated gradient needed for a FODO at 3 MeV and 352.2 MHz would be reliably achievable. The transition between the two focusing schemes is smooth and no emittance growth is observed, providing the matching is done adequately. A scheme with a FODO configuration on all the three tanks has been studied giving some advantages with respect to sensitivity to beam errors and it can be accommodated at any time in the linac design without modifications of the tank structure.

After the initial optimisation, a campaign of end-to-end simulations with the purpose of identifying bottlenecks, weak points and acceptance limitations, allowed a fine tuning of the layout. The codes PATH [14] and TRACEWIN [15] have been used with the following beam distributions [16], [17], [18], [19]:

- Generated test beam at the input of the DTL used to test the structures without space charge (50000 particles, 3 MeV, 352.2 MHz, I=0 mA).
- Generated DTL input beam with space charge (I=65 mA).
- Matched beam from the Medium Energy Beam Transport Line (MEBT) with space charge (I=62 mA).

The results are presented in Table 2 and clearly indicate that the DTL structure is adequate for the input beam, in particular the choice of bore radius.

Table 2. Emittance growth and beam transmission in the Linac4 DTL.

		1. Test beam (0 mA)	**2. Test beam (65 mA)**	**3. Beam from the MEBT Line (62 mA)**
Input Emittance (RMS, Norm.)	ε_X (π mm mrad)	0.28	0.28	0.33
	ε_Y (π mm mrad)	0.28	0.28	0.28
	ε_{long} (π deg MeV)	0.17	0.17	0.16
Output Emittance (RMS, Norm.)	ε_X (π mm mrad)	0.28	0.31	0.34
	ε_Y (π mm mrad)	0.28	0.30	0.32
	ε_{long} (π deg MeV)	0.17	0.18	0.18
Emittance Growth	ε_X (%)	0	10.7	2.5
	ε_Y (%)	0	7.1	12.8
	ε_{long} (%)	0	5.8	12.6
Transmission	%	100	100	100

Technologies

There are several viable solutions successfully used for building Drift Tube Linacs and usually the method of choice depends on the technological requirements, the available budget, as well as on the existing local expertise. The method described here refers to the Linac4 DTL, and could probably be adopted for the RAL linac project.

The mechanical design of the DTL aims at reducing the complexity of the mechanical structure and of the adjustment procedure. Drift tubes and holders on the tanks that are machined to tight tolerances do not require adjustment mechanisms like screws or bellows for drift tube positioning. A scaled cold model, an assembly model and a full-scale prototype of the first half section have been constructed to validate the design principles (Figure 4).

The DTL cavities consist of a steel cavity and girder, drift tubes assembled from pre-machined copper pieces, and accessories for mounting drift tubes in girders as well as for tuning, stabilization, support, vacuum pumping and alignment of the structures. The manufacturing process can be summarised as follows:

- Stainless steel cylinders are being used, machined and copper plated.
- There is only one weld for the cooling circuit of the RF port carried out before plating.
- The aluminium girders are precision machined for each drift tube and stainless steel rings are inserted into the openings from above and below.
- The drift tubes are assembled from pre-machined forged OFE copper with permanent magnet quadrupoles inserted inside the drift tubes. The assembly of the drift tube with stem is done by e-beam welding. After the cooling circuit has been vacuum tested, the drift tube is closed by e-beam welding to be done with magnetic field nearby.
- The positioning mechanism consists of a number of mechanical parts.
- Assembly is straightforward with an installation rate of 10 drift tubes per day.
- Tooling is required for keeping tolerances and all pieces have to be checked at the metrology lab.

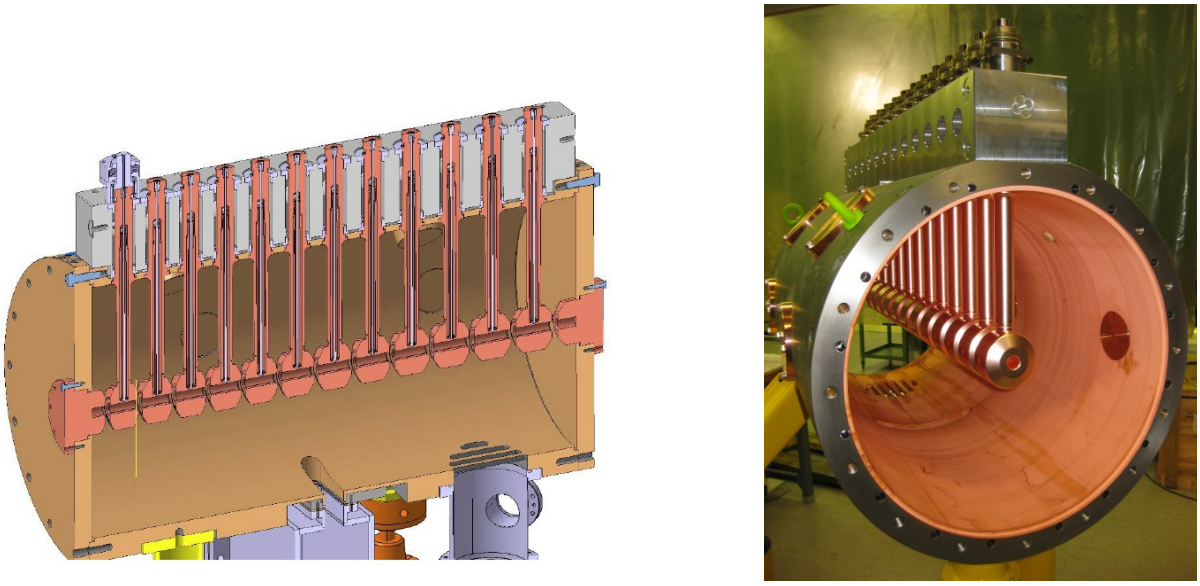

Figure 4. The CERN Linac4 DTL prototype.

The required alignment tolerances were defined by error studies on beam dynamics. Limits for transversal and rotational positioning of quadrupoles are tight. The longitudinal magnet position is less critical. The tolerances are stringent but following advances in machining quality, they are considered feasible without any further adjustment mechanism. In consequence, all critical parts have to undergo metrology before assembly [20], [21], [22], [23].

Table 3. Alignment tolerances in the DTL

Error Type	Maximum Amplitude
Transverse Drift Tube Displacements	$\delta_{X,Y}$ = ± 0.1 mm
Magnet Rotations	$\Phi_{X,Y,Z}$ = ± 0.3 mrad

Tuning

From the RF point of view, the DTL has been divided into three tanks, the first being 3.5 m long, whereas the other tanks are made of two mechanical sections of about the same length of tank 1, but connected to form two tanks of about 7 m length, in order to minimise the number of transitions.

Precise adjustment of the field in the tanks is provided by fixed tuners (5 for the first tank and 10 for each of the following tanks). One movable tuner per tank section keeps the tanks on frequency during operation. Post-coupler stabilisation is foreseen in the three tanks (9 post-couplers in tank 1, 16 in tank 2 and 23 in tank 3), although it is made more difficult by the small drift tube diameter leaving a distance of 1.01 $\lambda/4$ between the tank and the drift tube surface This a value considered the limit for achieving an effective stabilisation, but on the other hand this design profits from a higher shunt impedance [20].

A detailed 3D analysis of the post-coupler modes has been performed, indicating that, even for a configuration consisting of one post-coupler every three drift tubes in tank 1, stabilisation can be achieved.

A field flatness of ±1% is also achievable, although beam dynamics simulations indicate that more relaxed requirements are acceptable.

Sensitivity to RF Errors

The sensitivity to RF errors in Linac4 has been studied by tracking a Gaussian distribution containing 50000 particles over 500 runs, with random errors uniformly distributed. Two different types of dynamic errors (“Klystron errors”) have been applied: an error in RF phase and an error in amplitude. These errors appear at the RF power source level (3 for the DTL), are applied coherently to all RF gaps powered by the same source and cannot be cured.

Table 3 presents the impact of the klystron errors on the beam phase, energy jitter and RMS emittance at the end of the DTL. Values between ± 0.5 % and ± 2% for the amplitude and values between ±0.5 and ±2 degrees for the phase have been considered. From the results one can deduce that the amplitude errors have more impact than the phase errors and that a variation of ±2% in amplitude causes an emittance growth and an energy jitter above what is tolerable. A

control of the amplitude and phase within ±0.5% and ±0.5 degrees would be ideal, but ±1% and ±1 degree is also acceptable [24], [25].

Table 4. Results of dynamic error studies for the DTL (RMS quantities).

Errors: $E_{klystron\ [\%]}$, $\Phi_{klystron\ [deg]}$	**Phase Jitter [deg] 1 sigma**	**Energy Jitter [keV] 1 sigma**	**RMS emittance [deg.MeV]**
Nominal	-	-	0.167
± 0.5% - 0.5 ±deg	0.8	13	0.169±0.003
± 0.5% - ±1deg	0.9	18	0.171±0.004
± 0.5% - ± 2deg	1.1	31	0.175±0.009
± 1% - ± 0.5deg	1.6	23	0.1707±0.005
± 1% - ± 1deg	**1.6**	**28**	**0.1719±0.006**
± 1% - ± 2deg	1.8	36	0.1772±0.011
± 2% - ± 0.5deg	5.1	43	0.179±0.014
± 2% - ± 1deg	5.7	46	0.180±0.017
± 2% - ± 2deg	8.6	49	0.187±0.024

3.2. The Crossbar H-Mode DTL - CH-DTL

Over the last decades, several H-mode type cavities have been proposed for different applications. The Crossbar H-mode DTL (CH-DTL) is a new multi-cell drift tube cavity recently developed at IAP Frankfurt, operating in the TE210 mode (H210). The structure has good properties, with high shunt impedance, high accelerating fields and a compact design. It is well suited for pulsed high intensity proton and ion linacs covering the low and medium energy range from 5 to 150 MeV and it is the base for the new 70 MeV proton linac for the GSI FAIR project [26]. Although there is little operational experience with this structure, its RF properties are better than those of classical linac structures covering the same energy range and at the moment it is being analyzed as an option for the future accelerators, like the new proton booster at Fermilab or the IFMIF and EUROTRANS facilities.

RF Properties and Power Efficiency

The CH-DTL is an interesting alternative to the classical E-mode cavities and it is essentially an extension of the well established Interdigital H-cavities to higher frequency. The CH-DTL operates in Pi-mode and is characterised by the lack of internal focusing elements which allows the construction of extremely compact cavities having a higher shunt impedance when compared to conventional RF structures. In addition, such cavities can stand high RF fields in routine operation due to the small surface of the drift tubes.

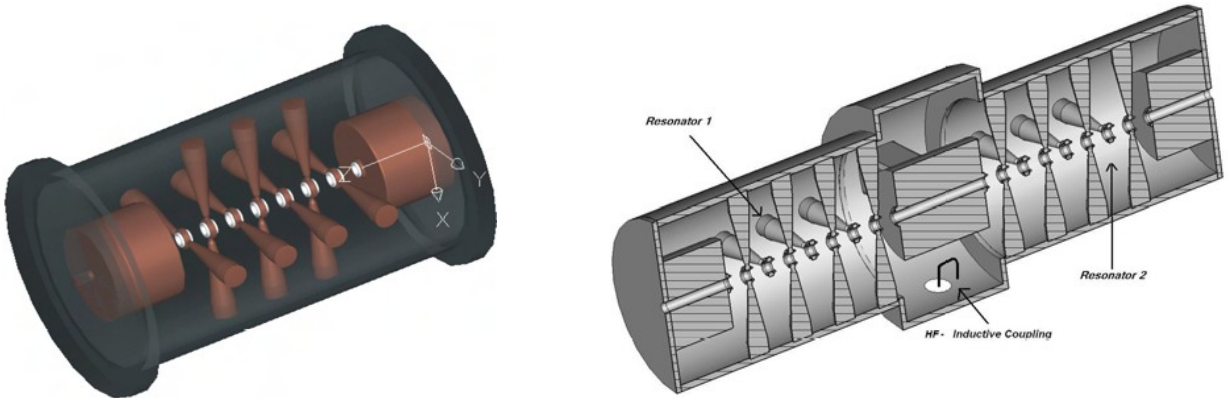

Figure 5. The CH-DTL structure: a single module (left) and coupled structure (right). The axial accelerating electric field is produced by orientating two neighbouring stems at 90° one against the other.

The FAIR proton injector at GSI will employ 12 CH-DTL type cavities with a variable number of gaps operating at 325 MHz, to accelerate a 70 mA proton beam (35 mA in the first stage) from 3 to 70 MeV. In order to match the klystron power level, the cavities are grouped in 6

pairs of coupled structures. Each resonator consists of 2 CH cavities connected by an intertank section which hosts a magnetic lens for transverse focusing and which distributes the input power between the accelerating structures (Figure 5). Three coupled resonators accelerate the beam up to 35 MeV where a dedicated diagnostics section will be positioned while the final acceleration up to 70 MeV will be done by the last three coupled resonators. The total length of the CH-DTL section of the linac is 23 m and the average accelerating gradient per cavity varies from 3 to 8 MV/m [27]. A summary of the RF properties of the CH-DTL can be seen in Table 5.

Table 5. CH-DTL RF Properties

	CH-DTL
Energy Gain (MeV)	3 – 70
Total RF Peak Power / Copper Power (MW)	10.1/5.32
E_0 (MV/m)	3 – 8
ϕ_s (deg)	- -45, -35, -30, 0
Maximum surface electric field (Kilp)	2
Frequency (MHz)	325
“Real estate” gradient (MV/m)	2.91
RF Power/Energy Gain (kW/MeV) – without beam loading	80
ZTT (MOhm/m)	40 – 95
Total Length (m)	23

The geometry of the structure has been optimised for high shunt impedance by means of 3D EM modelling using CST Microwave Studio. It has been observed that the stems are not only responsible for the mechanical stability of the structure, but they also carry the highest current density and provide the accelerating axial electric field, so for this reason their design merits special attention. Initially based on the existing IH structure but modified for the crossbar geometry, the shape of stems has eventually evolved into a conical profile with two cylinders. In order to preserve the efficiency of the structure the size of the stems has been carefully reduced so that the capacitive load between each pair of stems would be also decreased [28].

The effective shunt impedance variation along the FAIR linac can be seen in Figure 6. The theoretical results predicted by simulation codes have been verified by RF measurements on a

test model build at Frankfurt University and a reduction in shunt impedance of ~5% has been observed. The values in Figure 6 have been already scaled to take this result into account.

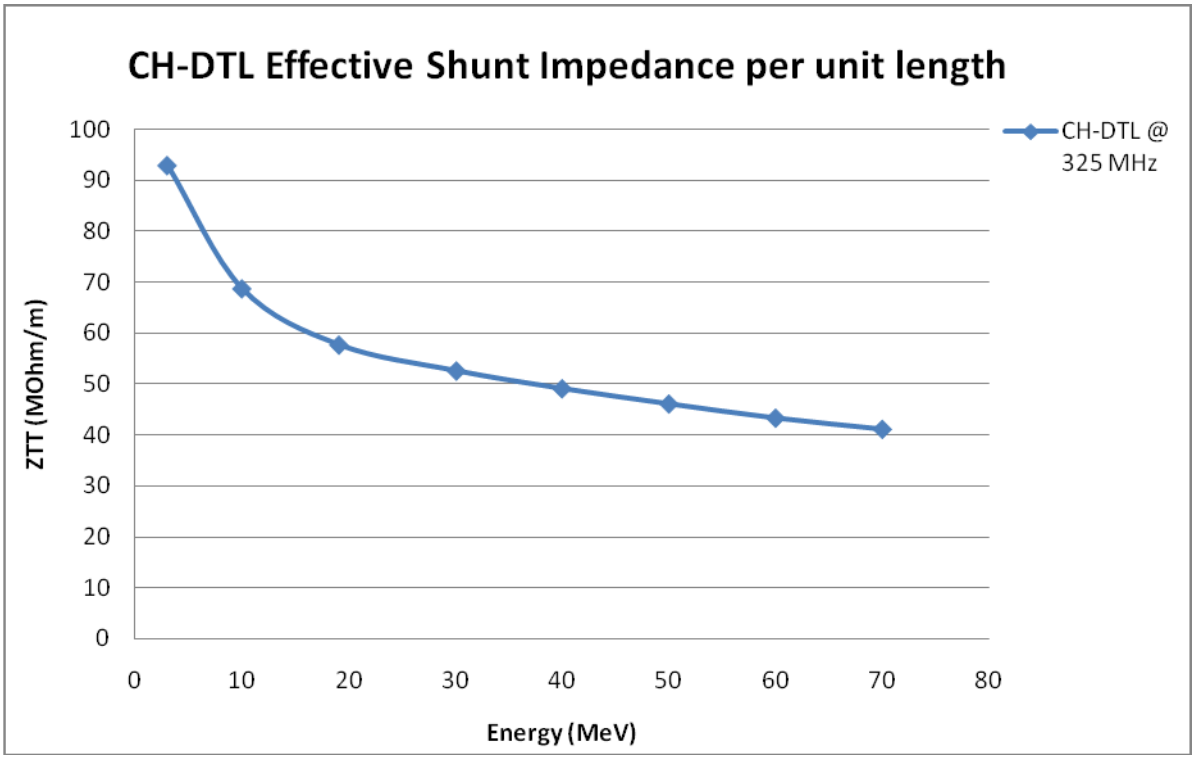

Figure 6. Effective Shunt Impedance per unit length for the CH-DTL structure.

Beam Dynamics

The beam dynamics design of the FAIR proton injector, is based the KONUS [29] lattice and has been performed using the LORASR Code. The KONUS beam dynamics scheme is an alternative focusing system devised at Frankfurt University and it essentially consists of the following elements:

- A quadrupole triplet for transverse focusing.
- A short negative synchronous phase structure for longitudinal focusing and matching (usually the first few gaps of the resonator).
- A long 0° structure with asynchronous beam injection that provides the main acceleration with transversal defocusing (most gaps of the resonator).

Due to the fact that the transverse focusing period is much longer than in a classical FODO structure normally used at low energies in a DTL, in order to avoid beam loss, the length of the first tank is limited to 10 gaps. Following the KONUS scheme, the first 3 gaps operate at -30° synchronous phase to bunch the beam, while the following 7 gaps operate at 0° and provide

the main acceleration up to ~6 MeV. At this point a magnetic quadrupole triplet is used to focus the beam transversally. The second section of the coupled CH-DTL resonator consists of 3 bunching gaps (-35°) followed by the 9 gaps operating at 0°. The following modules follow a similar pattern.

Table 6 presents the RMS emittance growth along the linac when tracking a beam (35 mA, 325 MHz, 4000 particles) generated with PARMTEQ and transported through the FAIR RFQ. Although the transmission is 100%, a high emittance growth is observed in both transverse and longitudinal planes. This beam behaviour is caused by the space charge forces at lower energies together with the necessity of keeping the dimension of the beam as small as possible in order to reduce the probability of losses. Also, due to the large input emittance in the longitudinal plane, the design aim was to minimize the emittance growth in this plane, which corresponds to an increase in the transverse planes [27].

Table 6. Emittance growth and beam transmission in the FAIR CH-DTL linac.

		RFQ Output (35 mA)
Input Emittance (RMS, Norm.)	ε_X (π mm mrad)	0.39
	ε_Y (π mm mrad)	0.38
	ε_{long} (π deg MeV)	0.1836
Output Emittance (RMS, Norm.)	ε_X (π mm mrad)	0.61
	ε_Y (π mm mrad)	0.61
	ε_{long} (π deg MeV)	0.2995
Emittance Growth	ε_X (%)	56
	ε_Y (%)	60
	ε_{long} (%)	63
Transmission	%	100

Technologies

In order to validate the theoretical results and test the fabrication steps and technical solutions involved in building the CH-DTL, a test model has been build at Frankfurt. The experience gained in manufacturing the model has been further used to construct a complete coupled resonator for the FAIR proton injector (the second coupled module).

The fabrication steps involved can be summarised as follows [27], [30].

- The double walled (for cooling) outer tank will be built from stainless steel and copper plated, resulting in a substantial cost saving. The girder initially proposed in one of the early design stages has been completely removed as there were concerns that welding this long bar onto the cylinder might have deformed the external structure.
- The stems, like the outer cylinder are also made from stainless steel. They are directly welded onto the tank from inside and then the whole structure is copper plated. The design of the stems aims for RF efficiency as well as mechanical stability in order to reduce the potential misalignment of the drift tubes. As a result the half geometry features a central ring (to attach the drift tubes), followed by a conical geometry ending with a cylinder that will be joined to the outer tank.
- The drift tubes are made from bulk copper and will be inserted in the central ring of the stainless steel stems using the “press fit technique” (the drift tubes are cooled down and inserted in the central ring. The successive thermal expansion will create a strong contact between the two). However, the deformation in the stems induced by the welding has had a detrimental impact on the RF contacts and as a result this method has been abandoned and the drift tubes will be welded onto the stems.

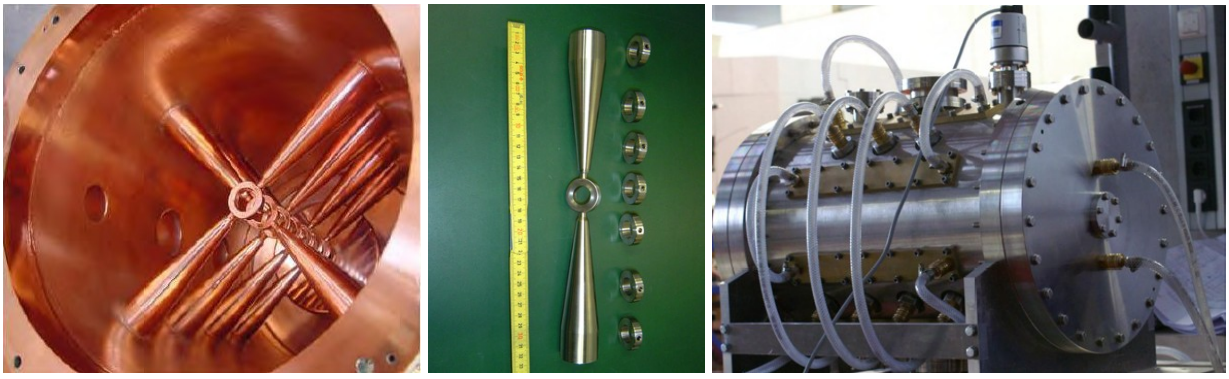

Figure 7. A copper plated CH-DTL cavity (left), stem (middle) and an assembled module with its cooling system.

Tuning

The CH-structure can be locally tuned by varying the gap/period length ratio. This is done using drift tubes with different lengths. Local gap voltage changes in the range ±20% can be achieved. Initially, the “press fit technique” was proposed to connect the drift tubes to the stems, but as explained above this method was abandoned and the tubes will be welded instead.

In order to approximate the zero-mode, the end cells are being used. Their resonant frequency is decreased by lengthening the last half drift tube and therefore increasing the

volume of the cell. In addition it is also possible to increase the radius of the last half drift tube inducing a strong capacitance with the closest stem. Using this method a 25% increase in the electric field in the last cell has been achieved.

In addition, for normal operation mobile tuners will also be used. Two-three tuners per cavity depending on the number of cells will provide the required degree of field and frequency tuning. Simulations and RF tests indicate that a field flatness of ±1-2% is achievable [27].

Sensitivity to RF Errors

Phase and voltage errors from amplifiers have been investigated in the FAIR linac to determine the tolerances for mechanical construction and the required RF control during operation. Like for the Linac4 structures, a ±1% error in amplitude and a ±1deg error in phase have been randomly generated at the klystron level (6 klystrons in total). Table 7 presents the RMS emittance growth with respect to the nominal case as well as the probability that the degradation of the emittance due to errors is within 1% or 5%. 1000 runs have been performed for each individual error with a Gaussian distribution containing 100000 particles. The conclusions of this study was that a ±1deg error in phase was tolerable but due to the distinctive characteristics of the KONUS focusing scheme, a reduction in voltage is not desirable, that is why the design aims for a +0.2% error in voltage at the klystron level [31].

Table 7. Results of dynamic error studies for the CH-DTL (RMS quantities).

Errors: $E_{klystron\ [\%]}$, $\phi_{klystron\ [deg]}$	**$\lvert\Delta\varepsilon_x/\varepsilon_x\rvert$ Probability**	**$\lvert\Delta\varepsilon_y/\varepsilon_y\rvert$ Probability**	**$\lvert\Delta\varepsilon_z/\varepsilon_z\rvert$ Probability**
± 1%	<5% 80.3 <10% 96.9	<5% 82.3 <10% 97.8	<5% 60.5 <10% 80.6
± 1deg	<5% 100	<5% 97.4 <10% 100	<5% 67.1 <10% 87.6

3.3. The Cell-Coupled Drift Tube Linac – CCDTL

At linac energies above 40 MeV alternative structures to the conventional drift tube linac can be used providing comparable energy efficiency with simpler construction and alignment. Different designs have been considered, all based on short DTL-like tanks containing only a few empty drift tubes, with quadrupoles placed externally between tanks. The main advantage of these structures is their lower price per meter as compared to a DTL, whose cost is dominated by the complex construction and alignment of the drift tube-quadrupole assembly and by the machining, handling and plating costs of the long DTL tanks. For structures with external quadrupoles, the drift tube alignment tolerances are much less demanding than for a DTL, and a good shunt impedance can be maintained while profiting of the adjustability of the electromagnetic quadrupoles. However, placing quadrupoles outside of the accelerating structure increases the length of the focusing periods and the maximum tolerable phase advance per period sets a lower limit to the energy at which these structures can be used [32].

RF Properties and Power Efficiency

For the new Linac4 injector at CERN a CCDTL operating at 352.2 MHz has been designed for an energy range between 50 and 102 MeV. The CCDTL has first been proposed at Los Alamos National Laboratory, and it operates in π-mode between the gaps in the tank and in π/2 mode between the tanks [33]. This structure is basically composed by several 3-gaps Alvarez structures (accelerating cells) coupled together by a small off-axis coupling cavity located at the equator of the accelerating cells (Figure.8). A set of 3 accelerating cells and 2 coupling cells forms a “module” which will be fed by a single klystron.

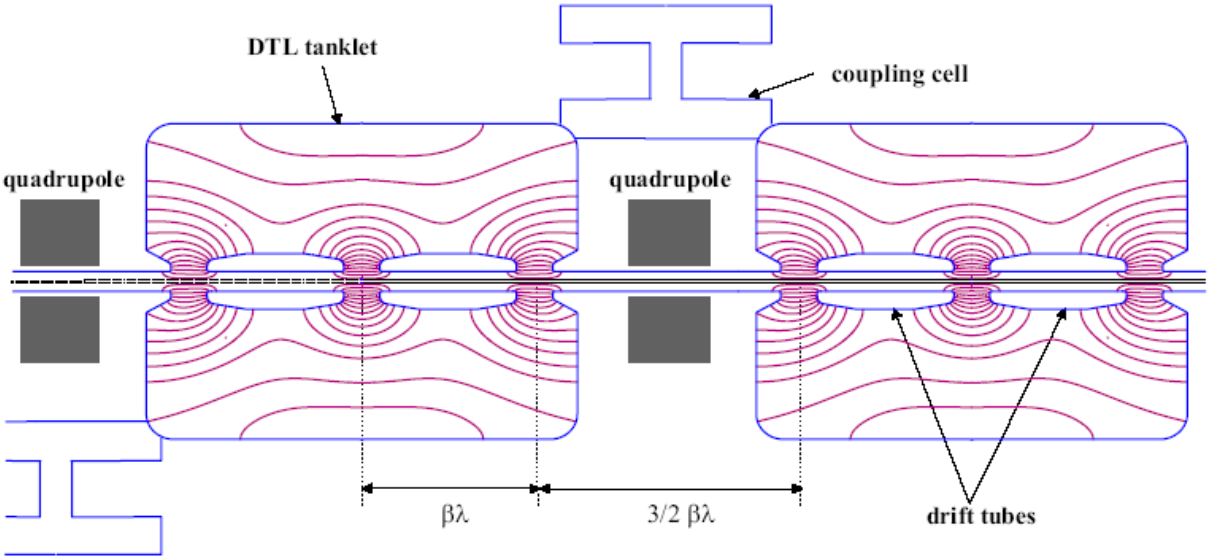

Figure 8. The CCDTL scheme.

The CCDTL section consists of 21 accelerating cavities grouped in 7 modules. Each accelerating cavity houses 2 drift-tubes and three gaps. Two full-scale prototypes of the CCDTL structures have been produced to validate the technology of the construction and successfully tested at high power.

Initial simulations were performed in order to maximize the shunt impedance by changing the cavity diameter, constant for the whole CCDTL section in order to simplify the geometry. The effective shunt impedance decreases rapidly with the particle velocity. This is the reason why around 100 MeV Linac4 has adopted a different accelerating structure. The constant diameter does not compromise the efficiency of the design because one can find a diameter which is still in the optimum range for all particle velocities. Similarly all other geometric parameters were analyzed in order to maximize the shunt impedance and at the same time to have a maximum Kilpatrick factor of 1.7 (high power test demonstrated that a Kilpatrick value of 1.8 was reached within a few days of conditioning). The RF properties of the CCDTL are given in Table 8. All power values were scaled by 1.2 to account for additional losses with respect to simulations. The losses on end walls, stems and coupling slots have been taken into account. Consistently the ZTT values are multiplied by a factor of 0.83 [34], [35], [36], [37].

Table 8. CCDTL RF Properties.

	CCDTL
Energy Gain (MeV)	50 – 102
Total RF Peak Power / Copper Power (MW)*	6.96/4.83
E_0 (MV/m)	4 – 4.4
ϕ_s (deg)	-20
Maximum surface electric field (Kilp)	1.7
Frequency	352.2
"Real estate" gradient (MV/m)	2.2
RF Power*/Energy Gain (kW/MeV) – without beam loading	93
ZTT* (MOhm/m) – Min/Max	32 - 41
Length (m)	23.4

* Calculated ZTT values scaled down to 83% to take into account additional losses. Consistently, the power dissipation values have been scaled up by a factor of 1.2.

The effective shunt impedance per unit length over the considered energy range can be seen in Figure 9 (un-scaled and scaled). The sudden increase in ZTT is due to the fact that the first three modules have been designed for a lower Kilpatrick filed, thus compromising the efficiency of the structure. Shunt impedance calculations have also been performed for the SDTL (Separated Drift Tube Linac) structure type operating at 324 MHz. The Separated Drift Tube Linac uses independently driven DTL tanks, with quadrupoles in between the tanks. This structure offers a high shunt impedance if the number of gaps per tank is sufficiently large and is currently being used at J-PARC in Japan to accelerate an H^- beam from 50 to 190 MeV.

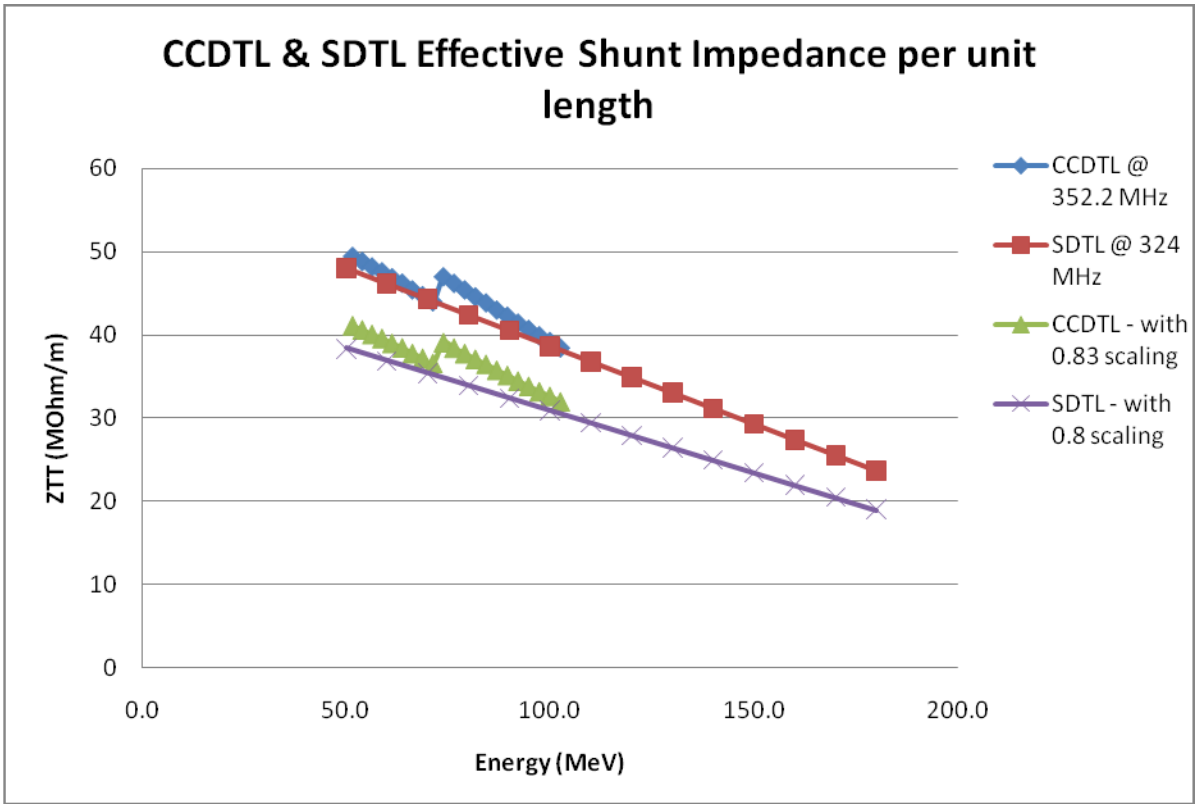

Figure 9. Effective Shunt Impedance per unit length for the CCDTL and the SDTL structures.

Beam Dynamics

At 50 MeV the beam is energetic enough to allow the transition to the CCDTL, a structure which doesn't follow the beam velocity profile cell-by-cell. The average synchronous phase in each tank is -20° and the focusing period is 3βλ. At the transition between tanks when one or more gaps are missing, the phase of the neighbouring cavities is adjusted to cope with the transition and to insure a smooth variation of the longitudinal phase advance. The same beam dynamics design approach already described in the DTL section has been used for the CCDTL sector of Linac4 [7]. Three different input distributions have been used with the following characteristics:

- Generated test beam at the input of the CCDTL used to check the structure without space charge (45000 particles, 40 MeV*, 352.2 MHz, I=0 mA).
- Generated test beam at the input of the CCDTL with space charge (I=65 mA).
- Matched beam from the DTL with space charge (I=62 mA).

* the input energy is 40 MeV due to the fact that in one of the early design stages the CCDTL structure was projected to cover the 40 to 90 MeV energy range.

The simulation results are presented in Table 9 and are characterised by a very small emittance growth and 100% transmission indicating a good choice of parameters for the CCDTL. [17], [19].

Table 9. Emittance growth and beam transmission in the Linac4 CCDTL section.

		1. Test beam (0 mA)	**2. Test beam (65 mA)**	**3. Beam from the DTL (62 mA)**
Input Emittance	ε_X (π mm mrad)	0.33	0.33	0.34
	ε_Y (π mm mrad)	0.32	0.32	0.32
	ε_{long} (π deg MeV)	0.17	0.17	0.18
Output Emittance	ε_X (π mm mrad)	0.33	0.32	0.34
	ε_Y (π mm mrad)	0.32	0.33	0.32
	ε_{long} (π deg MeV)	0.17	0.17	0.18
Emittance Growth	ε_X (%)	0	-3	-1.1
	ε_Y (%)	0	3	1.7
	ε_{long} (%)	0	0	0.8
Transmission	%	99.99	100	100

Technologies

Two “hot” prototypes have been built to verify the electromagnetic and mechanical design of the CCDTL cavities. One short model was built at CERN. It consists of two half tanks, closed with copper plated lids at the position of the electric symmetry plane in the tanks, and one coupling cavity. The second model was built at VNIITF and BINP in Russia.

Each CCDTL cavity is assembled out of two copper-plated (30 um) stainless steel half-tanks. The half-tanks for the series production will be machined out of pre-shaped stainless steel “buckets”. For the prototypes the half-tanks were made of discs and cylinders, which were then electron-beam welded around the circumference with full penetration of the weld for the CERN prototype, whereas for the ISTC prototype discs and cylinders were TIG (Tungsten Inert Gas) welded before the final machining. The pre-shaped raw material (the “bucket-shape”) is around 10% more expensive, but the savings in machining and welding time, together with the

improved material properties of the half-tanks justify the additional initial expense. A smooth surface on the inside of the tank, instead of a machined welding, reduces risk of porosities under the copper plating in the welding area and improves vacuum characteristics. Cooling channels are machined into the external part of the tanks. Each half-tank contains one drift tube, which is machined out of solid copper and which is cooled via the supporting copper stem.

The drift tubes are electron beam welded to the stem and then fixed on a girder, which is fixed on top the tanks. The alignment and fixing mechanism of the stem will be adapted from the CERN DTL design and it relies on the machining precision of the stem holder. This means that there is no possibility to change the alignment of the stems, other than re-machining the stem holder. Since there are no quadrupoles inside of the drift tubes, the required alignment precision for the stem is much less critical than for a DTL. The welding between the stem and the drift tube is a critical item because it defines the perpendicularity of the ensemble and thus the alignment precision of the drift tube in the tank, but techniques that decouple the problem of perpendicularity from the welding process are being developed [7], [21], [37].

Tuning

The modeling of a single module has been performed through circuit analysis using the PSpice code. The analysis calculates the field error introduced by frequency errors in each resonant cavity. These errors can be classified in two types: static error (resulting from residual tuning errors) and dynamics errors (i.e. caused by the change in the external temperature, or variation of the cooling water temperature or flow).

Using this model, a maximum of 0.2% tilt sensitivity of the voltage with respect to the average voltage has been calculated when assuming a residual frequency error of ±20kHz distributed randomly in each cell (static errors).

The frequency change due to a temperature variation of 10 °C is estimated to be lower than 50kHz. This variation is applied to both accelerating and coupling cells. In order to retune the cavity to 352.2MHz (the working mode) a tuner will be used in the accelerating cavity, in the middle of the module. The tuner frequency variation necessary to match the correct resonant frequency of the $\pi/2$-mode is equal to 150kHz. This will create a maximum voltage error in the accelerating cavities with respect to the average value of 0.4%. This is fully acceptable from the beam dynamics point of view and in conclusion, only one motorized tuner is necessary for each CCDTL module [22], [37].

Sensitivity to RF Errors

Equivalent RF error studies to those performed for the DTL structure have been done for the CCDTL. Just like for the DTL, the results (Table 10) confirm the Klystron's amplitude and phase should be controlled ideally to 0.5 % and 0.5 deg to control energy and phase jitter at the CCDTL output, but values of 1% and 1 deg are still acceptable [24], [25].

Table 10. Results of dynamic error studies for the CCDTL (RMS quantities) – 5000 runs.

Errors: $E_{klystron\ [\%]}$, $\phi_{klystron\ [deg]}$	**Phase Jitter [deg] 1 sigma**	**Energy Jitter [keV] 1 sigma**	**RMS emittance [deg.MeV]**
Nominal	-	-	0.196
± 0.5% - ± 0.5deg	0.5	39	0.196±0.003
± 1% - ± 1deg	1	63	0.196±0.005
± 2% - ± 2deg	2	115	0.198±0.009
± 5% - ± 2deg	4	237	0.200±0.015

3.4. The Side-Coupled Linac – SCL

Above ~ 90 MeV the shunt impedance of drift tube based structures like DTL or CCDTL starts to decrease rapidly, and the only option to maintain a high acceleration efficiency is to pass from structures operating in the 0-mode (0° phase difference between adjacent gaps on the beam axis) to structures operating in π-mode, which present a shunt impedance increasing with energy. At the same time, the reduced bunch length at high energy due to phase damping allows the increase of the RF frequency, with a further gain in shunt impedance and the possibility to operate at higher gradients. However, the smaller cell dimensions impose a drastic change in the mechanical construction technique, passing from the bolted units made out of copper-plated stainless steel to modules composed of smaller brazed full copper cells.

RF Properties and Power Efficiency

The Side-Coupled Linac structure was developed in 1967 at the Los Alamos National Laboratory and then used in most high-energy linacs projects worldwide (Los Alamos, Fermilab, SNS). Its peculiarity is that in addition to accelerating cells it also contains coupling cells, placed sidewise (Figure 10). From the beam point of view, this is a sequence of accelerating gaps operating in the π-mode (180° phase difference between cells), spaced by a distance βλ/2 in order to keep the synchronism between particles and accelerating field. From the RF point of view, it is a bi-periodic chain of resonators (accelerating and coupling cells) operating in the π/2 mode. In this mode, fields in adjacent cells have a 90° phase difference, all coupling cells have zero fields, while the accelerating cells are excited with the correct polarity.

For Linac4 the SCL was foreseen to accelerate the particles from 90 to 160 MeV, but later it was decided to be replaced by the Pi-mode structure. However, within the HIPPI collaboration, important contributions have been made to the development of this structure mostly by CERN, LPSC and INFN-Napoli. The operating frequency is 704.4 MHz, twice that of the DTL and the CCDTL. The SCL linac section is composed of tanks, each containing 11 accelerating cells and 10 coupling cells placed on alternating sides of the accelerating cells. The cells are magnetically coupled by slots at the intersection between accelerating and coupling cells. Electromagnetic quadrupoles are placed between tanks, and in order to form a continuous RF structure the quadrupoles are bridged by off-axis 3-cell coupler units. For a maximum klystron output power of 4MW, 5 tanks can be connected to form a module of 117 coupled cells fed by a single klystron [38], [39].

The basic cell design follows the same optimization procedure already described for the DTL and the CCDTL, taking into account different geometrical parameters. The aperture radius

affects significantly the shunt impedance; however, a relatively large value is required to provide a sufficient margin against halo particles loss when operating at high average currents. An approximate cost analysis indicates that an accelerating gradient of 4 MV/m corresponds roughly to the minimum of structure and RF cost and has been assumed as the design gradient for the SCL. At this gradient, the peak surface field is not a critical parameter, and the simulations show that the maximum electric field level is always kept below 1.2 Kilpatrick [7]. A summary of the RF properties of the SCL is presented in Table 11.

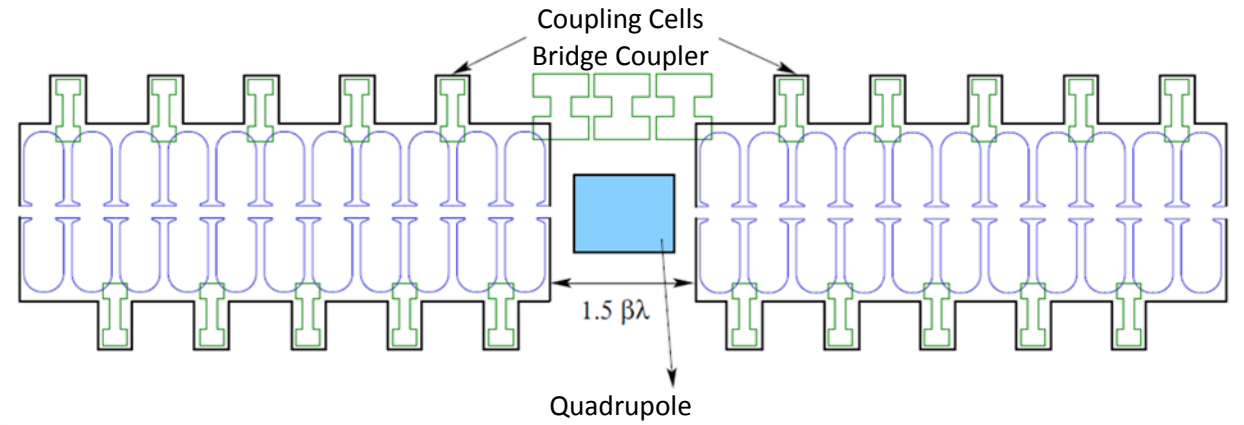

Figure 10. Scheme of two SCL tanks with quadrupole and bridge coupler.

Table 11. SCL RF Properties.

	SCL
Energy Gain (MeV)	90 – 160
Total RF Peak Power / Copper Power (MW)*	12.5/9.7
E_0 (MV/m)	4
ϕ_s (deg)	-20
Maximum surface electric field (Kilp)	1.2
Frequency	704.4
"Real estate" gradient (MV/m)	2.56
RF Power*/Energy Gain (kW/MeV) – with beam loading	140
ZTT* (MOhm/m) – Low DC/High DC (Min - Max)	34 – 40 / 29 - 36
Length (m)	20

* Calculated ZTT values scaled down to 80% to take into account additional losses. Consistently, the power dissipation values have been scaled up by a factor of 1.25.

In addition to the power calculations performed for the SCL structure, an extensive set of simulations have been carried out for two other best knows and widely used π/2-mode standing wave structures: the Annular Ring Coupled Structure (ACS) and the On Axis Coupled Structure (OCS) (Figure 11). The OCS was not considered as a suitable option since cooling is not possible without a significant reduction in ZTT [40].

An SCL cavity operating at 648 MHz currently being considered as an option for the RAL linac has also been analysed. The effective shunt impedance variation for the ACS, the CERN SCL and the RAL SCL operating at low duty cycle (thin walls (5 mm) that do not allow cooling channels) and high duty cycle (thick walls (15 mm) with cooling), is presented in Figure 12. The theoretical values have been scaled by a factor of 0.8 to account for additional losses.

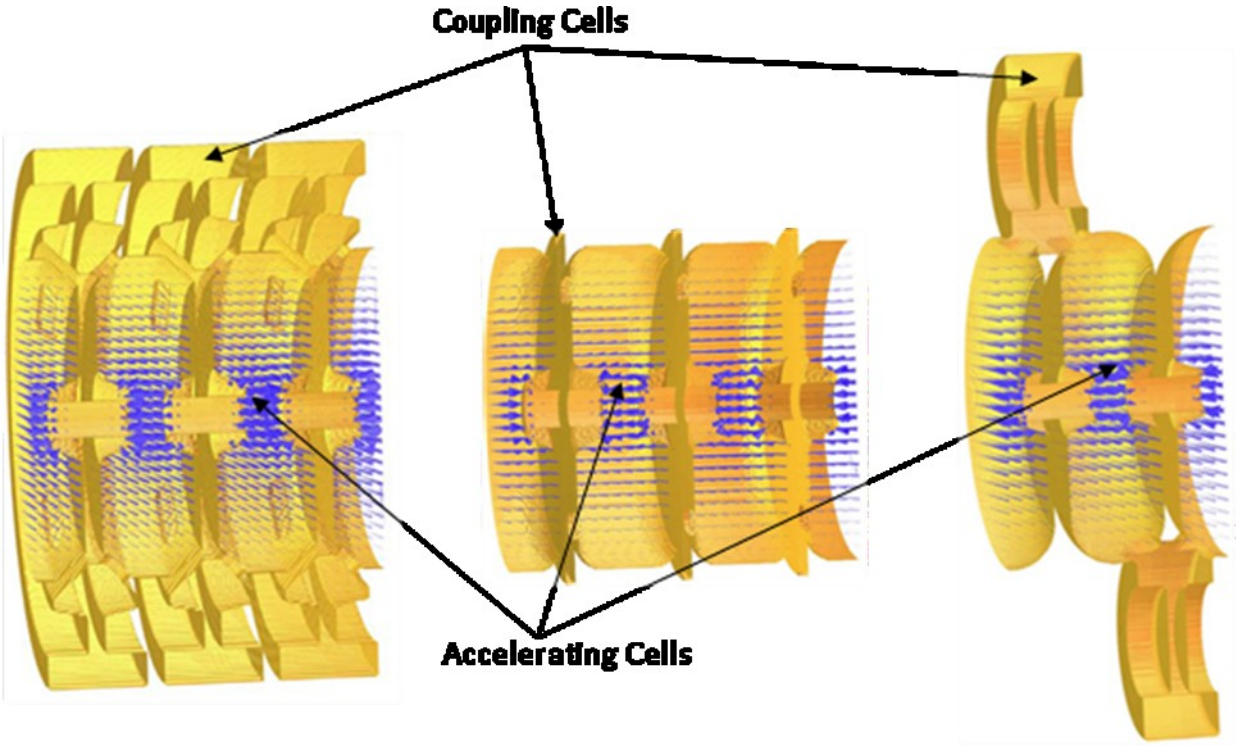

Figure 11. The ACS (left) the OCS (middle) and the SCL (right) structures.

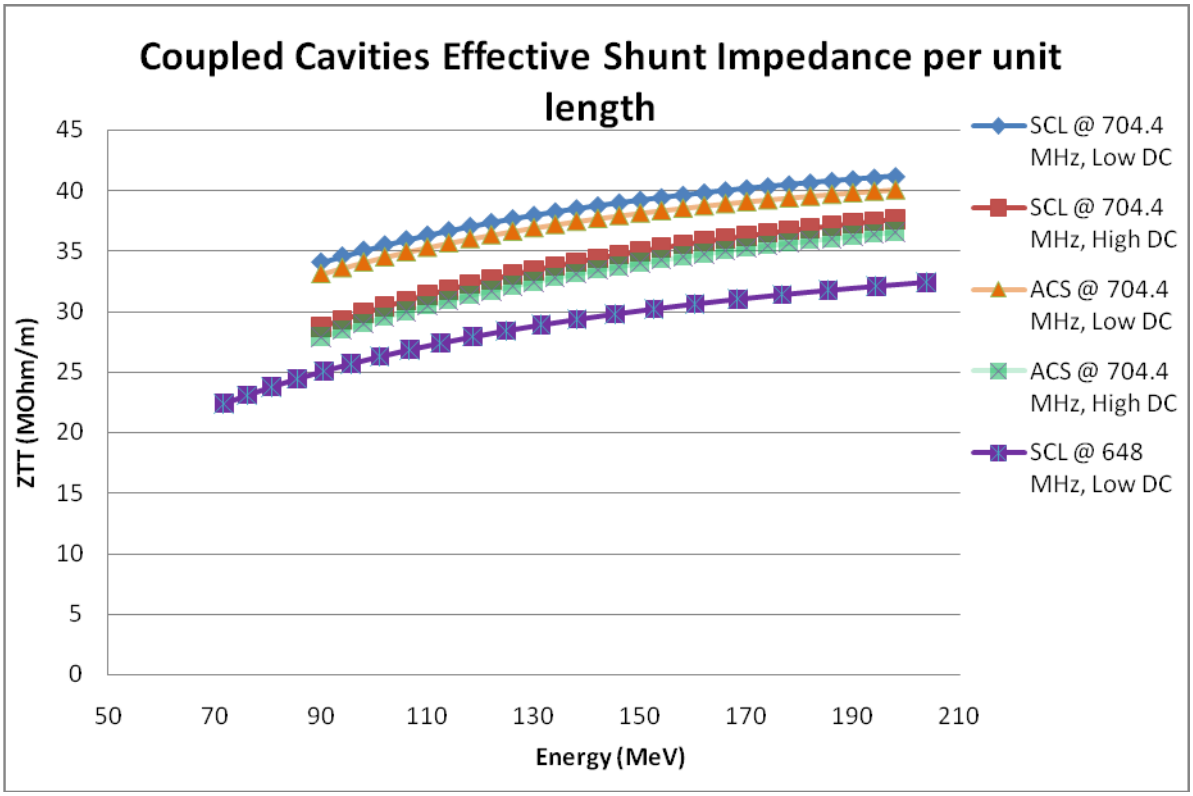

Figure 12. Effective Shunt Impedance per unit length for the SCL structure.

Beam Dynamics

Like the CCDTL, the SCL adopts a conventional FODO lattice, with quadrupoles placed between tanks. The SCL operates at 704.4 MHz, twice the frequency of the preceding structures and since the beam current used in the simulations is defined per RF frequency, the beam current in the SCL simulations had to be doubled as well (130 mA with every second RF bucket filled). A tune ratio $\sigma_l/\sigma_t \sim 0.7$ was retained in order to obtain a strong transverse focusing and a smaller transverse beam size while operating in a stable region close to equipartitioning. The variation of the longitudinal phase advance due to the frequency jump is controlled by adjusting the phase in the modules at the transition. The resulting phase advances are varying smoothly and do not give rise to emittance growth.

The beam dynamics simulations have been performed up to 180 MeV when the Linac4 injects in the SPL, and 160 MeV, the PS Booster injection energy. The results reported here refer to the 180 MeV simulations. In order to check the structure, the first runs have been done with a generated input beam. Once the structure has been checked simulations have been performed with the beam coming from the CCDTL [7], [16].

- Generated test beam at the input of the SCL used to check the structure without space charge (50000 particles, 90 MeV, 704.4 MHz, I=0 mA).
- Generated test beam at the input of the SCL with space charge (I=130 mA).
- Matched beam from the CCDTL with space charge (I=124 mA).

The simulation results are presented in Table 12.

Table 12. Emittance growth and beam transmission in the Linac4 SCL section.

		1. Test beam (0 mA)	2. Test beam (130 mA)	3. Beam from the CCDTL (124 mA)
Input Emittance	ε_X (π mm mrad)	0.30	0.30	0.34
	ε_Y (π mm mrad)	0.30	0.30	0.32
	ε_{long} (π deg MeV)	0.37	0.37	0.37
Output Emittance	ε_X (π mm mrad)	0.30	0.31	0.34
	ε_Y (π mm mrad)	0.30	0.32	0.33
	ε_{long} (π deg MeV)	0.38	0.38	0.37
Emittance Growth	ε_X (%)	0	-3.3	-0.1
	ε_Y (%)	0	6.6	4.3
	ε_{long} (%)	2.7	2.7	2.7
Transmission	%	100	100	100

Technologies

The construction techniques of the SCL differ from those of DTL and CCDTL because of the higher frequency and smaller size. The SCL cells are machined out of solid copper blocks, and then all cells in a tank are piled up and furnace brazed. RF tuning of the individual cells is required before brazing, and then the complete tank can be tuned to frequency and residual field errors corrected by applying deformation tuning of the cells. This construction and tuning technology is commonly used for this type of structures, and was successfully applied at CERN [] and SNS. At the LPSC Laboratory in Grenoble (France) an SCL cold model was built in order to study its RF properties and optimise the tuning strategy. A technological model of the SCL, made of two copper half-cells brazed together, has also been built in BINP (Novosibirsk). [41]

Tuning

The $\pi/2$ mode is intrinsically stable against perturbations coming from mechanical errors, beam loading etc., meaning that the longitudinal field distribution remains flat even in presence of asymmetries between cells. Stabilisation is obtained because modes around the $\pi/2$ give equal and opposite contributions from perturbations, finally cancelling out.

Tuning of a Side-Coupled Structure corresponds to setting the frequency of the accelerating cells equal to that of the coupling cells, which in turn consists of closing the stop-band in the dispersion curve of the bi-periodic structure. When the structure is correctly tuned, the accelerating and coupling cell passbands in the dispersion diagram are brought to a confluence and as a result, all modes contributing to perturbations, i.e. all the modes on the dispersion curve around the operating $\pi/2$ mode, will appear in pairs equally spaced around the $\pi/2$ mode. In presence of a "perturbation" (small asymmetry in the chain of resonators), the new ("perturbed") field will be a linear combination of all modes in the dispersion curve, but modes from the upper and lower branches of the dispersion curve will give equal contributions with opposite sign, finally cancelling out in accelerating cells.

In practice, the tuning is being done by iteratively machining a tuning ring inside each accelerating cell until a value slightly lower than the accelerating mode frequency has been achieved. The next step is to create a full cavity assembly from stacked accelerating and coupling cells and a second fine tuning is being performed first on the coupling cells (by squeezing or expanding the cell across the noses) and then on the accelerating cavities (by deforming the wall of each cell at special predesigned thinned areas on the side of the cell). []. Additional mechanical tuners are also being used. New methods for tuning the field level in the cavities have been developed by LPSC and INFN-Napoli. Theoretical calculations indicate that a field flatness of ±1.5% can be achieved for a coupling of 5% [42], [43].

Sensitivity to RF Errors

As described in the previous sections the sensitivity to klystron errors (there are 5 klystrons foreseen for the SCL) has been assessed. The effect these errors on the beam phase, energy jitter and RMS emittance at the end of the SCL can be seen in Table 13 [7], [24].

Table 13. Results of dynamic error studies for the SCL (RMS quantities).

Errors: $E_{klystron\ [\%]}$, $\phi_{klystron\ [deg]}$	**Phase Jitter [deg] 1 sigma**	**Energy Jitter [keV] 1 sigma**	**RMS emittance [deg.MeV]**
Nominal	-	-	0.18
± 0.3% - ± 0.3deg	0.6	73	0.1827±0.0036
± 0.6% - ± 0.6deg	1.12	144	0.1926±0.036
± 1% - ± 1deg	1.92	239	0.2106±0.0324

3.5. The Pi-Mode Structure – PIMS

The PIMS is an axisymmetric structure, operating in π-mode. Each cavity is made of multiple identical cells with off-axis coupling holes. This structure has been recently chosen to replace the Side Coupled Linac which was originally foreseen for the high energy section of Linac4. Although the PIMS has a smaller shunt impedance than the SCL it allows the operation of the linac at only one frequency (no frequency jump necessary) and its simple design and ease of manufacturing is expected to reduce the overall cost of the linac. The PIMS is based on the LEP expertise and makes use of all mechanical solutions developed for the LEP cavities [44].

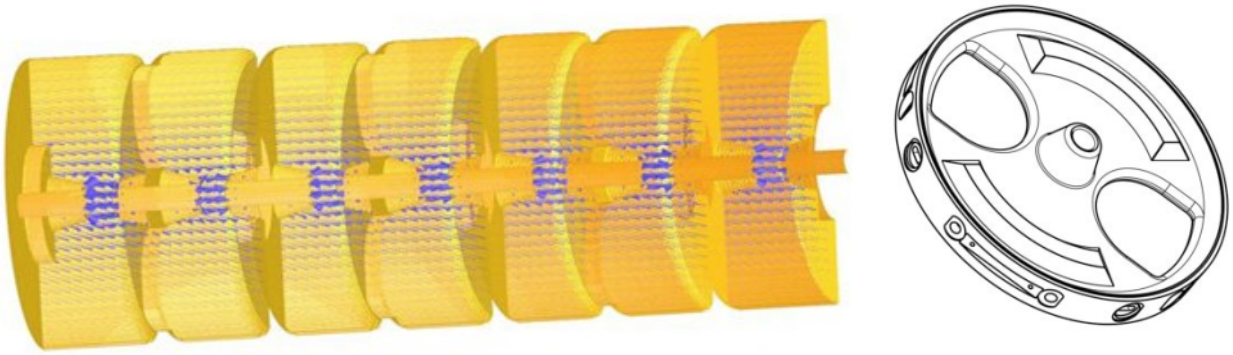

Figure 13. The PI-Mode Structure: the seven-cell structure (left) and the 3D disk geometry (right).

RF Properties and Power Efficiency

The PIMS will cover the 102 to 160 MeV energy range in Linac4 and it uses 84 cells (12 cavities of 7 cells) operating at 352.2 MHz. This is an advantage compared to the previous design employing the SCL structure which was projected to use a total of 468 cells (220 accelerating cells plus coupling cells) operating at 704.4 MHz to accelerate beam from 90 to 160 MeV. The basic PIMS design is a scaled version of the normal conducting LEP accelerating structure modified for a medium β operation and a higher cell to cell coupling.

The accelerating gradient in the first 10 cavities has been adjusted to a relatively high value of 4 MV/m, resulting in a maximum power of ~1MW per cavity. Using a high gradient, limits the number of cells per cavity to 7, and thus makes it easier to obtain a flat field distribution. The last 2 cavities are used not only for acceleration but also for energy painting for injection into the subsequent Proton Synchrotron Booster (PSB). In order to achieve a high ramping speed in these cavities, the nominal accelerating gradient was lowered to 3.1 MV/m [45]. The basic design was made with Superfish and the 3D calculations to determine the coupling coefficients,

shunt impedance degradation (due to coupling, tuners, etc), and end-cell tuning were made with GdfidL [46]. An overview of the main parameters is given in Table 14.

Table 14. PIMS RF Properties.

	PIMS
Energy Gain (MeV)	102 – 160
Total RF Peak Power / Copper Power (MW)	11.3/8.97
E_0 (MV/m)	4
ϕ_s (deg)	-20
Maximum surface electric field (Kilp)	1.8
Frequency	352.2
"Real estate" gradient (MV/m)	2.63
RF Power/Energy Gain (kW/MeV) – without beam loading	155
ZTT (MOhm/m) - Low DC/High DC (Min - Max)	27 – 29 / 23 – 26
Total Length (m)	22

* Calculated ZTT values scaled down by 30% to take into account additional losses. Consistently, the power dissipation values have been scaled up by a factor of 1.42.

After the geometry of the basic PIMS cell has been optimised, an extensive set of shunt impedance simulations has been performed, investigating two different wall thicknesses: a thicker wall that allows cooling channels and a thinner wall for low duty cycle operation. In addition, a comprehensive analysis of the effects that generate additional losses has been carried out. These effects, including the surface roughness, wave guide coupler, e-beam welding groove, tuning rings and tuners, account for a ~19.5 % reduction in shunt impedance. The enlarged volume of the end cells generates an increase of ~ 4% in shunt impedance, but on the other hand for a 5% coupling, the coupling slots account for a further ~12.5% reduction. For Linac4 operation this means a total reduction of ~28%. For power calculations an additional safety margin is being used and the calculated values are scaled by 30%. This is significantly higher than the scaling used for the other structures which take into account only 20% additional losses [45]. The effective shunt impedance per unit length over the considered energy range can be seen in Figure 14 (scaled and un-scaled).

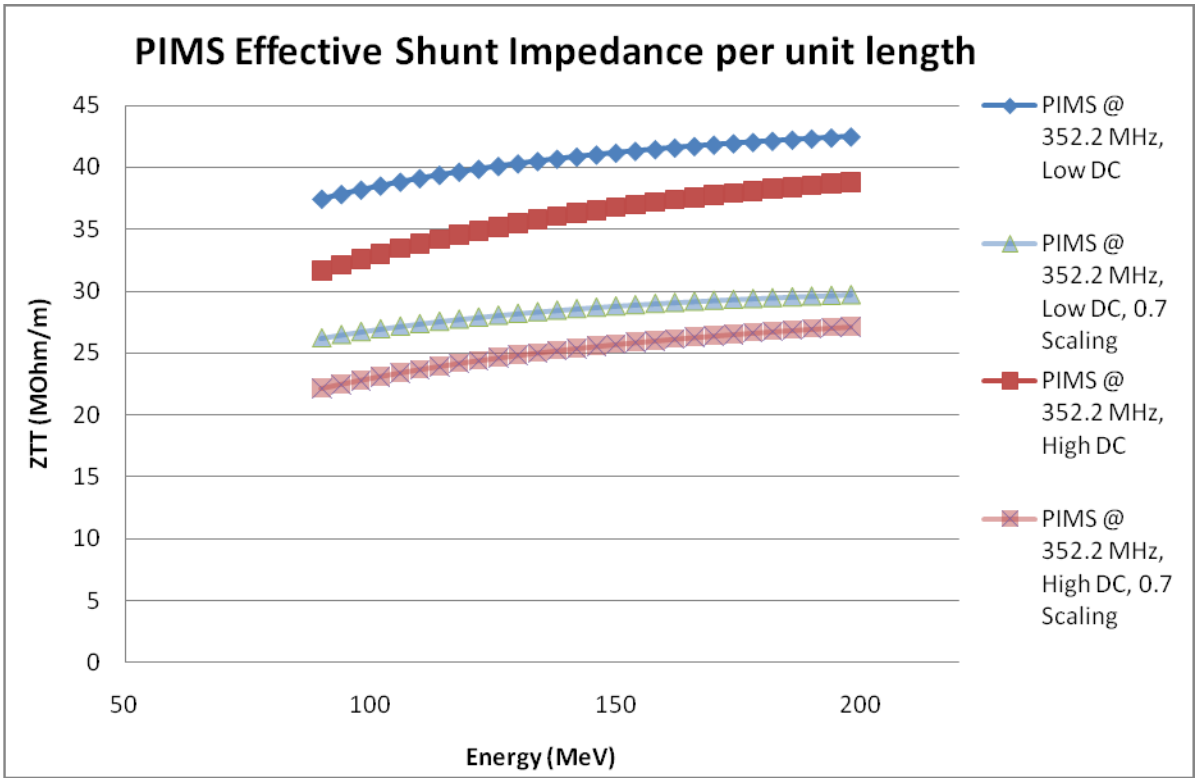

Figure 14. Effective Shunt Impedance per unit length for the PIMS structure.

Beam Dynamics

An ample beam dynamics study comparing the PIMS operating at 352.2 MHz and the SCL at 704.4 MHz has been performed at CERN. In this comparison the SCL tanks consisting of 11 accelerating cells and 10 coupling cells are replaced by the 7-cell PIMS cavities. As a result the length of the focusing period is increased by ~30% and the resulting increase in beam size is compensated by increasing the aperture of the PIMS modules. Due to the elimination of the frequency jump, longitudinal matching between the preceding CCDTL and the PIMS becomes much easier. Simulations indicate that the beam dynamics performance and the beam quality are as good as in the SCL [47], [48]. Table 15 presents the transmission and the emittance growth when running the following beam distributions:

- Generated test beam at the input of the PIMS used to check the structure without space charge (50,000 particles, 100 MeV, 352.2 MHz, I=0 mA).
- Generated test beam at the input of the PIMS with space charge (I=58.72 mA).
- Matched beam from the CCDTL with space charge (I=58.72 mA).

Table 15. Emittance growth and beam transmission in the Linac4 PIMS section.

		1. Test beam (0 mA)	2. Test beam (58.72 mA)	3. Beam from the CCDTL (59 mA)
Input Emittance	ε_X (π mm mrad)	0.1610	0.1610	0.3219
	ε_Y (π mm mrad)	0.1563	0.1563	0.3169
	ε_{long} (π deg MeV)	0.1814	0.1814	0.1739
Output Emittance	ε_X (π mm mrad)	0.1611	0.1770	0.3301
	ε_Y (π mm mrad)	0.1564	0.1701	0.3167
	ε_{long} (π deg MeV)	0.1817	0.1950	0.1735
Emittance Growth	ε_X (%)	~0	~9.9	2.55
	ε_Y (%)	~0	~8.8	-0.06
	ε_{long} (%)	~0.2	~7.5	-0.23
Transmission	%	100	100	100

Technologies

The Linac4 PIMS cavity design is based on the Pi-mode 352 MHz LEP accelerating cavities, scaled for medium β operation. Many of these cavities were constructed by ACCEL and were reliably used during several years in LEP at CERN. All mechanical solutions were developed at CERN.

The structure consists of discs and cylinders that are machined out of solid OFE copper blocks. About 40% less copper is needed for the PIMS with respect to the SCL. Cooling channels are drilled from the outside into the discs so that any brazing or welding between vacuum and water can be avoided thus preventing any risk of water leaking into the vacuum of the cavity. Brazing is avoided and as a result, all copper ports including the RF, tuner and vacuum ports are electron-beam welded onto the cylinders. Seven cells are clamped together to form a cavity on which low level RF tests are being performed. The cavity is then reopened and the tuning rings are being machined. The procedure is repeated several times until the desired resonant frequency is reached and then the complete cavity is electron-beam welded.

The cells are coupled by two coupling slots, which are turned by 90 deg from cell to cell to minimise the second neighbour coupling. The geometry of the coupling slots has been analysed by means of 2D/3D EM modelling so that the optimum coupling coefficient is achieved and the losses are reduced. Three 3-cell and one 7-cell cold models have been build and measured at CERN in order to understand the simulation results and to verify the construction steps. This has confirmed that the overall design and the manufacture procedure is much simpler than for the SCL. The minimal tolerance is on the nose cone where a ±20 µm machining precision is required. For comparison, the SCL requires a ±10 µm precision in the same region [45], [49], [50].

A high power prototype of a complete 7-cell PIMS module is now under construction.

Figure 15. PIMS aluminium cold model.

Tuning

The frequency tuning of the structure is done in 2 stages. Before the joining of the discs and cylinders, the machined cells are clamped together and the cell frequencies are measured. Deviations are then corrected in one or several steps by re-machining the tuning rings, taking into account the expected frequency shifts due to vacuum, welding, heating, etc. The tuning rings are divided in two sections of 90° to avoid field disturbances in the coupling region and are expected to provide a rough tuning range between -1.5 and +1.0 MHz. A second, more accurate tuning is done using piston tuners placed in each cell. A fully penetrated tuner will increase the cell's frequency by 1 MHz. Tuners in cells 2 and 6 in the 7-cell PIMS module will be motorized to allow an active control of the resonant frequency and the field tilt, while all the other cells have fixed tuners, which are cut to length after the assembly of the complete cavities.

The aim is to achieve a range of ±25 kHz for the RF tuning, but even with a ±50 kHz range, a ±2.5% field stability can be achieved. Beam dynamics simulations indicate that a ±5% field stability is acceptable [45].

Sensitivity to RF Errors

The sensitivity to klystron errors has been analysed as already described for the previous structures. The results are presented in Table 16. The simulations confirm that klystron phase and amplitude should ideally be controlled to 0.5 % and 0.5 degree to control energy and phase jitter, but that a value of 1 % and 1 degree are still acceptable. For the PIMS the value of 1% and 1 degree is a hard limit, as the maximum energy jitter acceptable for a successful energy painting is 125keV (1 sigma value) [25].

Table 16. Results of dynamic error studies for the PIMS (RMS quantities).

Errors: $E_{klystron\ [\%]}$, $\Phi_{klystron\ [deg]}$	**Phase Jitter [deg] 1 sigma**	**Energy Jitter [keV] 1 sigma**	**RMS emittance [deg.MeV]**
Nominal	-	-	0.180
± 0.3% - ± 0.3deg	0.3	65	0.181±0.00088
± 0.5% - ± 0.5deg	0.4	78	0.181±0.00094
± 1% - ± 1deg	0.66	126	0.181±0.0012
± 2% - ± 1deg	0.85	220	0.181±0.0013

4. Comparison Tables

In this chapter, a summary of the properties for the five structures discussed above will be presented.

4.1. RF Properties and Shunt Impedance

Table 17. Summary of the RF properties for the HIPPI NC structures.

	Linac4 DTL	RAL DTL	CH-DTL	CCDTL	SCL	PIMS
Energy Gain (MeV)	3 – 50.2	3 – 74.8	3 – 70	50 – 102	90 – 160	102 – 160
Total RF Peak Power / Copper Power (MW)	4.72/2.82	7.67/5.52	10.1/5.32	6.96/4.83	12.5/9.7	11.3/8.97
E_0 (MV/m)	3.2	2.71 to 2.9	3 – 8	4 – 4.4	4	4
ϕ_s (deg)	-30 to -20	-42 to -21	-45, -35, -30, 0	-20	-20	-20
Maximum surface electric field (Kilp)	1.6	1.44	2	1.7	1.2	1.8
Frequency	352.2	324	325	352.2	704.4	352.2
"Real estate" gradient (MV/m)	2.5	1.96	2.91	2.2	2.56	2.63
RF Power/Energy Gain (kW/MeV) – without beam loading	60	76.8	80	93	140	155
ZTT (MOhm/m) – Min/Max	30-56	25 - 45	40 - 95	32 – 41	29 - 36	23 – 26
Total length (m)	18.7	36.6	23	23.4	20	22
Design Duty Cycle %	10	2.1	0.028	10	10	10

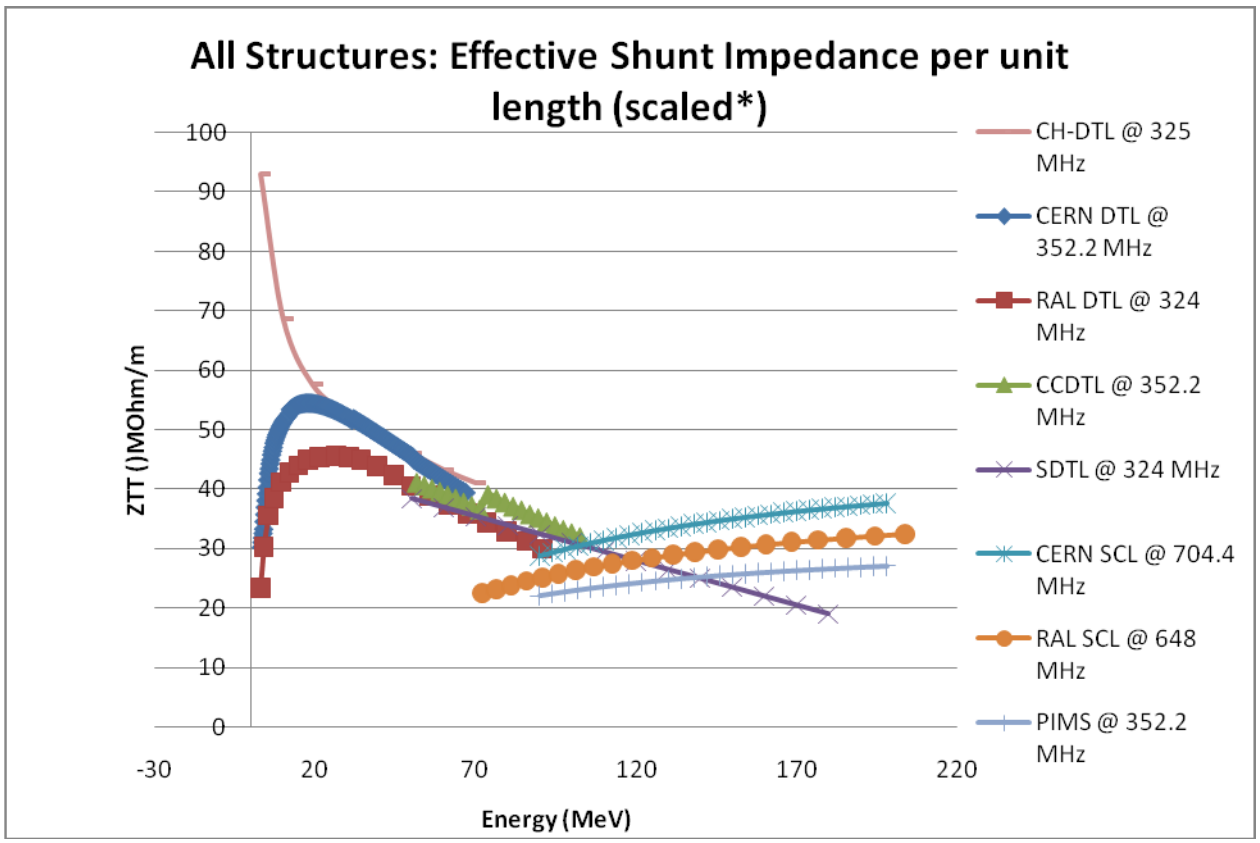

Figure 17. Effective Shunt Impedance per unit length for all structures.

* Calculated ZTT values scaled down to take into account additional losses. The following factors have been used:

DTL – a 20% reduction which doesn't include the contribution of the post-couplers.

CH-DTL – simulations in good agreement with measurements .A 5% reduction has been used.

CCDTL – a 17% reduction.

SCL – a 20% reduction.

PIMS – a 30% reduction.

4.2. Beam Dynamics

Table 18. Summary of the emittance growth and beam transmission in the HIPPI NC structures.

Structure	Distribution	Input Emittance (RMS, Norm.) X,Y (π mm mrad) Long (π deg MeV)	Output Emittance (RMS, Norm.) X,Y (π mm mrad) Long (π deg MeV)	Emittance growth (%)	Transmission (%)
DTL	Test Beam (0 mA)	ε_X = 0.28	ε_X = 0.28	0	100
		ε_Y = 0.28	ε_Y = 0.28	0	
		ε_{long} = 0.17	ε_{long} = 0.17	0	
	Test Beam (65 mA)	ε_X = 0.28	ε_X = 0.31	10.7	100
		ε_Y = 0.28	ε_Y = 0.30	7.1	
		ε_{long} = 0.17	ε_{long} = 0.18	5.8	
	Beam from the MEBT line (62 mA)	ε_X = 0.33	ε_X = 0.34	2.5	100
		ε_Y = 0.28	ε_Y = 0.32	12.8	
		ε_{long} = 0.16	ε_{long} = 0.18	12.6	
CH-DTL	RFQ Output (35 mA)	ε_X = 0.39	ε_X = 0.61	56	100
		ε_Y = 0.38	ε_Y = 0.61	60	
		ε_{long} = 0.1836	ε_{long} = 0.2995	63	
CCDTL	Test Beam (0 mA)	ε_X = 0.33	ε_X = 0.33	0	99.99
		ε_Y = 0.32	ε_Y =0. 32	0	
		ε_{long} = 0.17	ε_{long} = 0.17	0	
	Test Beam (65 mA)	ε_X = 0.33	ε_X = 0.32	-3	100
		ε_Y = 0.32	ε_Y = 0.33	3	
		ε_{long} = 0.17	ε_{long} = 0.17	0	
	Beam from the DTL (62 mA)	ε_X = 0 34	ε_X = 0.34	-1.1	100
		ε_Y = 0.32	ε_Y = 0.32	1.7	
		ε_{long} = 0.18	ε_{long} = 0.18	0.8	
SCL	Test Beam (0 mA)	ε_X = 0.30	ε_X = 0.30	0	100
		ε_Y = 0.30	ε_Y = 0.30	0	
		ε_{long} = 0.37	ε_{long} = 0.38	2.7	
	Test Beam (130 mA)	ε_X = 0.30	ε_X = 0.31	-3.3	100
		ε_Y = 0.30	ε_Y = 0.32	6.6	
		ε_{long} = 0.37	ε_{long} = 0.38	2.7	
	Beam from the CCDTL (124 mA)	ε_X = 0.34	ε_X = 0.34	-0.1	100
		ε_Y = 0.32	ε_Y = 0.33	4.3	
		ε_{long} = 0.37	ε_{long} = 0.37	2.7	
PIMS	Test Beam (0 mA)	ε_X = 0.1610	ε_X = 0.1611	0	100
		ε_Y = 0.1563	ε_Y = 0.1564	0	
		ε_{long} = 0.1814	ε_{long} = 0.1817	0.2	
	Test Beam (58.72 mA)	ε_X = 0.1610	ε_X = 0.1770	9.9	100
		ε_Y = 0.1563	ε_Y = 0.1701	8.8	
		ε_{long} = 0.1814	ε_{long} = 0.1950	7.5	
	Beam from the CCDTL (59 mA)	ε_X = 0.3219	ε_X = 0.3301	2.55	100
		ε_Y = 0.3169	ε_Y = 0.3167	-0.06	
		ε_{long} = 0.1739	ε_{long} = 0.1735	-0.23	

4.3. Technologies

Table 19. Summary of the technologies involved.

Technologies	DTL	CH-DTL	CCDTL	SCL	PIMS
Vacuum Sealing	- Helicoflex gaskets	Helicoflex Gaskets	- Helicoflex gaskets	Brazing	- E-beam welding
Surfaces	- Copper plating - OFE Copper	Copper plating	-Copper plating - OFE Copper	OFE Copper	- OFE Copper
RF Contacts	-Helicoflex seals	Helicoflex Seals	-Helicoflex seals	Brazing	-Helicoflex™ seals
Tolerances	- Precise machining* - Laser tracking	Precise machining	Precise machining	Precise machining	Precise machining
Focusing Elements	PMQ inside drift tubes	External/Internal EMQ triplet	External EMQs	External EMQs	External EMQs
Assembly	- E-beam welding (DT)	E-beam welding	- Brazing - E-beam welding (DT)	Brazing	- E-beam welding
Raw Cavities	- Cold drawn stainless steel tubes	Stainless steel	- Forged stainless steel	Forged OFE Copper	- Forged OFE Copper
Tuning	- Tuners	Mobile Plungers	- Tuners - Drift Tube Machining	- Dinging - Tuning ring machining	- Tuners - Tuning ring machining
Stabilization	- Post-couplers	No	Coupling cells	Coupling cells	- No

4.4. Sensitivity to RF Errors

Table 20. RF Errors in the DTL, CCDTL, SCL and PIMS.

Structure	Klystron errors (±1% Amplitude, ±1deg Phase)			
	Phase Jitter [deg] 1 sigma	Energy Jitter [keV] 1 sigma	Reference RMS Emittance [deg.MeV]	RMS emittance growth [deg.MeV]
DTL	1.6	28	0.1719±0.006	0.167
CCDTL	1	63	0.196±0.005	0.196
SCL	1.92	239	0.1926±0.036	0.180
PIMS	0.66	126	0.1810±0.0012	0.180

Table 21. RF Errors in the CH-DTL

Errors: $E_{klystron\ [\%]}$, $\phi_{klystron\ [deg]}$	$\lvert\Delta\varepsilon_x/\varepsilon_x\rvert$ **Probability**	$\lvert\Delta\varepsilon_y/\varepsilon_y\rvert$ **Probability**	$\lvert\Delta\varepsilon_z/\varepsilon_z\rvert$ **Probability**
± 1%	<5% 80.3 <10% 96.9	<5% 82.3 <10% 97.8	<5% 60.5 <10% 80.6
± 1deg	<5% 100	<5% 97.4 <10% 100	<5% 67.1 <10% 87.6

4.5. Cost Estimate

Estimating the cost involved in building accelerating structures is a complex task, requiring a detailed analysis of the cost for every component at various production stages. Cost parameters can change depending on many factors, but in general a rough estimate for an operational machine has to include the cost of the accelerating structure, support stand, vacuum systems diagnostics and the tunnel [4].

The design of the Linac4 and the FAIR proton injector took into account the impact of every design choice both on the capital and the operational costs. The shunt impedance for each structure type has been carefully optimised to increase the power efficiency while the technologies and the materials used, aimed for an optimum balance between cost and quality. A rough capital cost estimate can be seen in Table 22 for the DTL, CH-DTL, CCDTL and the PIMS. The SCL hasn't been included as its development stopped at an early design stage thus making a realistic cost approximation very difficult.

Table 22. General estimate of the capital costs involved in the construction of the accelerating structures for Linac4 and the FAIR linac.

Structure	Length (m)	Energy Gain (MeV)	Total Structure Cost (k€)	Cost/m (k€)	Cost/MeV (k€)	Obs.
DTL	~18.3	47	1953 k€ (2930 kCHF at 1€=1.5 CHF)	107 k€ (160 kCHF at 1€=1.5 CHF)	41 k€ (62 kCHF at 1€=1.5 CHF)	*
CCDTL	~20	52	2667 k€ (4000 kCHF at 1€=1.5 CHF)	133 k€ (200 kCHF at 1€=1.5 CHF)	52 k€ (78 kCHF at 1€=1.5 CHF)	
PIMS	~18.5	58	2547 k€ (3820 kCHF at 1€=1.5 CHF)	138 k€ (206.5 kCHF at 1€=1.5 CHF)	44 k€ (66 kCHF at 1€=1.5 CHF)	
CH-DTL	~2.2	12.5	345 k€	160 k€	28 k€	**

* The cost includes: support, power couplers, machining costs, materials (incl. joints, etc). It doesn't include: installation cost, prototyping, testing, manpower for tuning and RF measurements.

** These figures refer to module 2 only (tanks 3 and 4). The price includes the resonator (254 k€) and copper plating, plungers, tuning, RF-coupling, etc. (97 k€). In addition to this each module will be equipped with two triplets and their power supplies (248 k€). This brings the total cost for the accelerating structure and the transverse focussing elements to 599 k€ (254 + 97 + 248). This is equivalent to 48 k€/MeV or 272 k€/m.

5. Conclusions

In this report we present a comparative assessment of five normal conducting accelerating structures proposed for three future high intensity pulsed proton linacs: the Linac4 at CERN, the FAIR proton injector at GSI and the ISIS upgrade linac at RAL. The cavities operating in the 3 to 200 MeV energy range and at frequency between 324 and 704.4 MHz are: the DTL, CH-DTL, CCDTL, SCL and PIMS. The performance of each individual structure has been evaluated based on several criteria: RF properties and power efficiency, beam quality, technologies, tuning procedure and sensitivity to RF errors.

For the lower energy range (3 – 50 MeV) the DTL and CH-DTL structures are more suitable offering a high shunt impedance and an adequate beam dynamics. At linac energies above ~50 MeV alternative structures to the conventional drift tube linac, like the CCDTL, can also be used providing comparable energy efficiency with simpler construction and alignment. Above ~ 100 MeV the shunt impedance of drift tube based structures like DTL, CH-DTL or CCDTL starts to decrease rapidly, and the only option to maintain a high acceleration efficiency is to pass from structures operating in the 0-mode to structures operating in the π-mode, that present a shunt impedance increasing with energy like the PIMS and the SCL structures.

It is interesting to note that while some cavities appear to have superior characteristics, the final choice of a linac structure requires a complex analysis and depends on the particularities of each individual project. The operating frequency, the required duty cycle and beam current, the existing accelerators and infrastructure as well as the available local expertise all play an important role in the final decision. The objective of this report is to present an unbiased description of the work that has been done by different research groups within the HIPPI collaboration and it is not intended to present a hierarchy of accelerating cavities.

Acknowledgments

This report summarises the work done by our HIPPI colleagues who have contributed with portions of the text, calculations and many fruitful discussions. The HIPPI External Advisory Committee has also provided useful information and advice.

In addition, we acknowledge the support of the European Community-Research Infrastructure Activity under the FP6 "Structuring the European Research Area" program (CARE, Contract No. RII3-CT-2003-506395).

References

[1] R. Garoby, “High Intensity Pulsed Proton Injectors”, CARE Meeting, November 2003.

[2] J. Stovall, “Low and Medium Energy Beam Acceleration in High Intensity Linacs”, Proc. of EPAC’04.

[3] HIPPI Website, http://mgt-hippi.web.cern.ch/mgt-hippi/

[4] T. Wangler, “RF Linear Accelerators”, John Wiley & Sons, New York, 1998.

[5] W.D. Kilpatrick, “Review of Scientific Instruments”, vol. 28, p. 824, 1957.

[6] S. Ramberger et al., “Drift Tube Linac Design and Prototyping for the CERN Linac4”, CARE-Conf-08-025-HIPPI.

[7] F. Gerigk, M. Vretenar - editors, “Linac4 Technical Design Report”, CERN-AB-2006-084 ABP/RF (2006).

[8] F. Gerigk - editor, “Conceptual Design Report of the SPL II”, CERN-2006-006 (2006).

[9] C. Plostinar, “Progress on the RAL Linac Design”, HIPPI 2008 Annual Meeting, CERN, Geneva, October 2008.

[10] F. Gerigk, “A New 180 MeV H^- Linac for Upgrades of ISIS”, Proc. of EPAC’04, Lucerne, Switzerland, July 2004.

[11] Poisson Superfish, http://laacg.lanl.gov/laacg/services/download_sf.phtml

[12] CST Microwave Studio, http://www.cst.com/

[13] E. Sargsyan, A. Lombardi, “Consideration in Field Ramp for the Linac4 DTL Design”, CARE-Note-2008-003-HIPPI.

[14] A. Perrin, J.F. Amand, “Travel User Manual”, 2003.

[15] R. Duperrier, N. Pichoff, D. Uriot, “CEA Saclay Codes review for high intensity linacs”, Proc. of ICCS 2002, Amsterdam, 2002.

[16] A.M. Lombardi et al.,”End-to-End Simulations of Linac4”, CERN-AB-Note-2006-033.

[17] A.M. Lombardi et al., “End-to-End Beam Dynamics for CERN Linac4”, CERN-AB-2007-001.

[18] A.M. Lombardi et al., “Loss Control and Steering Strategy for the CERN Linac4”, AB-Note-2007-033-ABP.

[19] A.M. Lombardi et al., “Beam Dynamics in Linac4 at CERN”, HB2008, August 2008.

[20] S. Ramberger et al., “AN Optimised Design for the Linac4 Drift Tube Linac”, CARE-Report-08-054-HIPPI.

[21] F. Gerigk et al., “RF Structures for Linac4”, Proc. of PAC 2007, Albuquerque, NM, USA, June 2007.

[22] M. Vretenar et al., “Status of the Linac4 Project at CERN“, CARE-Conf-08-021-HIPPI.

[23] M. Vretenar, “Linac4 Status”, HIPPI 2008 Annual Meeting, CERN, Geneva, October 2008.

[24] M. Baylac et al., “Statistical Simulations of Machine Errors for Linac4”, Proc. of HB2006, Tsukuba, Japan.

[25] A.M. Lombardi et al., “Effects of RF Errors on the Linac4 Performance”, HIPPI 2008 Annual Meeting, CERN, Geneva, October 2008.

[26] D. Krämer, “FAIR – An International Facility for Antiproton and Ion Research”, Proc. of RuPAC 2006, Novosibirsk, Russia.

[27] G. Clemente PhD Thesis, “The Room Temperature CH-DTL and its Application for the FAIR Proton Injector”, Johann Goethe University, Frankfurt am Main, 2007.

[28] G. Clemente et al., “Geometrical Optimisation of the 70 mA, 70 MeV CH-Proton Injector Cavity for the FAIR Project”, GSI Annual Report 2004.

[29] R. Tiede et al., “KONUS Beam Dynamics Design of a 70 mA, 70 MeV Proton CH-DTL for GSI-SIS12”, LINAC ’04, Lubeck, pag. 60.

[30] G. Clemente et al., “Development of a Normal Conducting CH-DTL”, Proc. of PAC 2005, Knoxville, TN, USA, June 2005.

[31] G. Clemente et al., “Beam Dynamics Layout and Loss Studies for the Fair P-Injector”, Proc. of EPAC 2008, Genoa, Italy, June 2008.

[32] F. Gerigk, M. Vretenar, “Design Choices for the SPL Normal Conducting Front End (3 - 120 MeV), CERN-NUFACT-NOTE NF 110.

[33] J. Billen et al., “A New RF Structure for Intermediate-Velocity Particles”, LINAC ’94.

[34] M. Pasini, “CCDTL Design Update for Linac4”, CARE-Note-2005-014-HIPPI.

[35] M. Pasini et al., “CCDTL Prototype: Status Report”, CARE/HIPPI Document-2006-021.

[36] M. Pasini et al., “CCDTL Prototypes: Test Results”, CARE-Report-2007-036-HIPPI.

[37] M. Vretenar et al., “CCDTL Section for Linac4”, CARE/HIPPI Document-2008-020.

[38] E. Benedico Mora, M. Vretenar, “Design of a Side-Coupled Linear Accelerator Structure for Linac4”, CARE-Note-2005-015-HIPPI.

[39] M. Vretenar et al., “Design and Development of RF Structures for Linac4”, Linac ‘06, Knoxville, USA.

[40] R. Wegner, F. Gerigk, “A Comparison of Pi/2-Mode Standing Wave Structures for Linac4”, CERN-AB-Note-2006-049-RF.

[41] J.-M. De Conto et al., “Development of Side Coupled Cavities”, CARE-Note-08-11-HIPPI

[42] T. Clauser et al., “A New Tuning Method for Resonant Coupling Structures”, Proc. of PAC 2005, Knoxville, TN, USA, June 2005.

[43] N. Bultman et al., “Fabrication and Tuning of the SNS CCL Hot Model”, Proc. of PAC 2003, Portland, OR, USA, May 2003.

[44] I. Wilson, H. Henke, “The LEP Main Ring Accelerating Structure”, CERN-Report-89-09.

[45] F. Gerigk, R. Wegner, “PIMS – A Simple and Robust Accelerating Structure for High Intensity Proton Linacs”, Preprint submitted to Elsevier, January 2008.

[46] GdfidL, http://www.gdfidl.de

[47] E. Sargsyan, “Comparison of Beam Dynamics in SC Triple Spoke Cavities, triple-SCL and PIMS”, HIPPI Annual Meeting, September 2007, IPN, Orsay, France.

[48] E. Sargsyan, A. Lombardi, “Pi-Mode 352 MHz Scaled LEP Cavities as an Alternative Accelerating Structure for the Energy Range of 90 to 160 MeV in CERN Linac4/SPL”, CARE-Note-2007-003-HIPPI.

[49] R. Wegner, “PI-Mode Structure (PIMS)”, HIPPI 2008 Annual Meeting, CERN, Geneva, Switzerland, October 2008.

[50] P. Bourquin et al., “Development Status of the Pi-Mode Accelerating Structure (PIMS) for Linac4”, CARE-Conf-08-024-HIPPI.